Sauro S, Osorio R, Watson TF, Toledano M. Influence of phosphoproteins' biomimetic analogs on remineralization of mineral-depleted resin-dentin interfaces created with ion-releasing resin-based systems. Dent Mater. 2015 Jul;31(7):759-77. doi:10.1016/j.dental.2015.03.013.

Influence of phosphoproteins' biomimetic analogues on remineralization of mineral-depleted resin-dentin interfaces created with ion-releasing resin-based systems

Salvatore Sauro [a*], Raquel Osorio [b], Timothy F Watson [C], Manuel Toledano [b]

a – Dental Biomaterials and Minimally Invasive Dentistry, Departamento de Odontología, Facultad de Ciencias de la Salud, Universidad CEU-Cardenal Herrera, Valencia, Spain.

b – Dental Materials, School of Dentistry, University of Granada, Colegio Máximo, Campus de Cartuja, Granada, Spain

c – Biomaterials, Biomimetics & Biophotonics, King's College London Dental Institute at Guy's Hospital, London, UK

Key words: Biomimetic, Bioactive, Remineralization, Dentin, Bonding, Resin-based systems

Short title: Biomimetic remineralization of mineral-depleted resin-dentin interfaces

ACKNOWLEDGMENTS:

This work was supported by grant MINECO/FEDER MAT2014-52036-P.

***CORRESPONDING AUTHOR**

Prof. Dr. Salvatore Sauro

Dental Biomaterials, Minimally Invasive Dentistry and Dental Research Coordinator

Departamento de Odontología - Facultad de Ciencias de la Salud

Universidad CEU-Cardenal Herrera

46115 - Alfara del Patriarca, Valencia, Spain

ABSTRACT

Objectives. The study aimed at evaluating the remineralization of acid-etched dentin pre-treated with primers containing biomimetic analogues and bonded using an ion-releasing Ca-Silicate/CaP light-curable resin-based material.

Methods. An experimental etch-and-rinse adhesive system filled with Ca^{++}, PO_4^{-3}-relesing micro-fillers was created along with two experimental primers containing biomimetic analogues such as sodium trimetaphosphate (TMP) and/or polyaspartic acid (PLA). Dentin specimens etched with 37% H_3PO_4 were pre-treated with two aqueous primers containing the polyanionic biomimetic analogues or deionized water and subsequently bonded using the experimental resin-based materials. The specimens were sectioned and analyzed by AFM/nanoindentation to evaluate changes in the modulus of elasticity (Ei) across the resin-dentin interface at different AS storage periods (up to 90 days). Raman cluster analysis was also performed to evaluate the chemical changes along the interface. The phosphate uptake by the acid-etched dentin was evaluated using the ATR-FTIR. Additional resin–dentin specimens were tested for microtensile bond strength. SEM examination was performed after de-bonding, while confocal laser microscopy was used to evaluate the interfaces ultramorphology and micropermeability.

Results. Both biomimetic primers induced phosphate uptake by acid-etched dentin. Specimens created with the ion-releasing resin in combination with the pre-treatment primers containing either PLA and TMA showed the greatest recovery of the Ei of the hybrid layer, with no decrease in μTBS ($P>0.05$) after 3-month AS storage. The ion-releasing resin applied after use of the biomimetic primers showed the greatest reduction in micropermeability due to mineral precipitation; these results were confirmed using SEM.

Significance. The use of Ca-Silicate/CaP ion-releasing resin-based system applied to acid-etched dentin pre-treated with biomimetic primers containing analogues of phosphoproteins such as poly-L-aspartic acid and/or sodium trimetaphosphate, provide a suitable bonding approach for biomimetic remineralization of resin-dentin interfaces.

1. INTRODUCTION

Dental caries represents the major reason for placement and replacement of restorations [1,2]. The concept of minimally invasive (MI) was also applied for the treatment of deeper carious lesions by adopting the atraumatic restorative treatment (ART) approach (1990s) with the aim of selective caries removal to excavate infected carious tissue leaving as much caries-affected dentin as possible for therapeutic remineralization [3].

Contemporary ART concepts coupled with the advent of the latest generation of adhesive systems have radically influenced modern operative management of dental caries [4, 5]. The application of resin-based materials on demineralized dentin (e.g. acid-etched dentin) followed by placement of aesthetic light-curing resin-composites represents a revolution in adhesive dentistry [6, 7]. Acid-etching is the first step in resin-dentin bonding. Using 32-37% phosphoric acid in etch-and-rinse adhesive systems, this step removes smear layers and completely demineralizes dentin to a depth of 5-8 μm. That step also uncovers and activates all preforms of the endogenous proteases of dentin matrices metallo-proteinases (MMPs) and cathepsin, [8]. As the mineral phase of dentin is 50 vol% mineral, complete demineralization replaces all that minerals with 50 vol% of water. Because the proteases are hydrolases – that is, they hydrolyze peptide bonds by enzymatically adding water across specific peptide bonds, it is important that resins replace all of that water, so that the proteases cannot degrade collagen.

Unfortunately, resin-infiltration of water-saturated dentin matrices is not uniform, in particular in thick layers of caries-affected dentin. Indeed, some areas of hybrid layers are well-infiltrated and exhibit little residual water, while adjacent regions are not properly infiltrated and may contain very little resin, but 30-40% residual water [9, 10]. It is thought that the resin-sparse, water-rich zones in resin-bonded interfaces degrade over 1-2 years and their stiffness is so low that they may undergo excessive cyclic strain under normal function and fatigue failure [11].

Clinicians only have one chance for resin-infiltration. If normal resin-dentin bonds include 30-50% of their volume filled with water instead of resin, how can these water filled defects be corrected? One answer to that problem is to displace the residual water by filling the voids with nano-sized crystals of apatite. Remineralization is a form of dehydration [12, 13]. By removing residual water by remineralization, the activated MMPs in the matrix can be inactivated [13].

It has been recently proposed that all resin-bonds be covered with a flowable resin composite containing amorphous calcium phosphate (ACP)/calcium silicates/and biomimetic polyanions that can slowly diffuse through any water-filled channels (e.g. water trees in adhesives and hybrid layers, residual water in un-infiltrated dentin) and "back-fill" any such defects with apatite-like mineral crystals, displacing all residual water and inactivating all proteases by mineralizing the enzymes; this approach was shown to increase the durability of such resin-dentin bonds [14].

One more critical problem associated with such aesthetic restorations is the absence of therapeutic remineralization of caries-affected dentin and the poor durability/integrity of the resin–dentin interface during aging [15]. ART is considered to have a combined technique-material effect. It requires removal of the caries-infected dental tissues in order to arrest the caries progression (Massler's theory) and induces dental remineralization while utilizing the healing potential of glass ionomer cements (GICs) [2].

Unfortunately, Yiu *et al*. [16] demonstrated that, even though specific GICs developed for the ART treatments of carious dentin may favor the penetration of particular ions deep into caries-affected dentin [17, 18], they fail to remineralise apatite-depleted dentin due to a lack of nucleation of new apatite. This lack of remineralization has also been confirmed by Kim *et al*. [19] who reported the failure of GICs to remineralise apatite-depleted dentin, even in the presence of biomimetic remineralizing analogues. Also in this case, the application of biomimetic analogues as therapeutic

remineralizing strategies has been advocated as a possible method to achieve a more reliable approach to restore the elastic modulus values due to the creation of apatite crystallites similar to those of sound dentin [20-22]. The advent of these new therapeutic concepts in minimally invasive restorative/adhesive dentistry has captured the attention of many researchers so far, showing encouraging results both in terms of healing properties (i.e. remineralization) [23] and longevity of the bonding interface [24, 25]. Nevertheless, it is still necessary to generate bioactive/biomimetic strategies with enhanced therapeutic remineralization properties at the hybrid layer.

Thus, the present study aimed at evaluating the remineralizing of water-saturated collagen that remains uninfiltrated with resin when using an experimental light-curable resin-based etch-and-rinse dental adhesive containing ion-releasing micro-fillers applied on acid-etched dentin pre-treated with one of the different biomimetic primers containing either sodium trimetaphosphate [26] or polyaspartic acid as a nano-precursor cluster stabilizer [27]. The null hypothesis to be tested was that the pre-treatment of acid-etched dentin with biomimetic primers does not improve the remineralization ability of an experimental light-curable resin-based system containing ion-releasing micro-fillers.

2. MATERIALS AND METHODS

2.1 Preparation of the Experimental Resin and Biomimetic Primers

A control co-monomer blend (Res.CTR) was formulated using urethane dimethacrylate (UDMA: 30 wt%), ethoxylated bisphenol-A dimethacrylate (Bis-GMA: 5 wt%), triethyleneglycol dimethacrylate (TEGDMA: 25 wt%) (Esstech, Essington, PA) hydroxyethyl methacrylate (HEMA: 18 wt%), absolute ethanol (15 wt%), camphorquinone (CQ: 1.0 wt%), and ethyl-4-dimethylaminobenzoate (EDAB: 1.0 wt%) (Sigma-Aldrich, St. Louis, MO). A control primer (Pr.CTR) was also created by solvating Res.CTR (50 wt%) with absolute ethanol (50wt%). A type I Portland cement (Italcementi Group, Italy) (80 wt%) was mixed with 20 wt% β-TCP (Sigma-Aldrich) and deionized water (ratio 2:1). After setting (24 h), the cement was incubated at 40°C for 12 h, milled, sieved to <30 μm and incorporated as a filler

into the unfilled resin control (filler/resin ratio: 40/60 wt%) to create the experimental ion-releasing resin (Res.IR)[19].

The first biomimetic primer solution was created by dissolving 150 µg/mL of poly-L-aspartic acid (PLA) with a molecular weight of 27 KDa (Sigma-Aldrich) as previously described [27-28]. A second biomimetic primer solution (TMP+PLA) was created by dissolving 10 wt% sodium trimetaphosphate (TMP; Mw 367.8, Sigma-Aldrich), an analogue of dentin matrix proteins, and 150 µg/mL of PLA in deionized water; the pH of both solutions was adjusted to 7.1 [20, 26]. This experiment was designed to have the presence of such chemical species released by the bioactive ion-releasing filler and from the artificial saliva solution (AS) used in this study. The composition of artificial saliva was 0.7 mM/L $CaCl_2$, 0.2 mM/L $MgCl_2$, 4.0 mM/L KH_2PO_4, 30.0 mM/L KCl, 20.0 mM/L HEPES [23].

2.2 ATR-FTIR Analysis of Dentin Collagen

Six sound human third molars were obtained with informed consent from donors and used in accordance with the ethical guidelines of the Research Ethics Committee (REC) for medical investigations. The teeth were stored at 4 ^{o}C in 0.5% chloramine-T up to 30 days before use. Two middle-dentin specimens (2 x 2 x 1.5 mm) were obtained from each tooth using a hard tissue microtome (Accutom-50; Struers, Copenhagem, Denmark) equipped with a slow-speed water-cooled diamond wafering saw (330-CARS-70300, Struers, Copenhagen, Denmark). A 320-grit silicon carbide (SiC) abrasive paper mounted on a water-cooled polishing machine (LaboPol-4, Struers, Copenhagen, Denmark) was used to produce a clinically relevant smear layer on both surfaces of the specimens. The dentin specimens were immersed in a 37% H_3PO_4 solution and etched for 15 s; they were thoroughly rinsed with distilled water (5 s). These specimens (n^{o} sp. =2/each group) were used to evaluate the chemical changes (phosphate uptake) induced by the two experimental biomimetic primers compared to the single control primer (no biomimetic agents) when applied onto demineralized dentin for 1 min and subsequently rinsed with distilled water (5 s); etched-dentin specimens pretreated with deionized water were also analyzed. Three different positions of each specimen were analyzed using the ATR-FTIR Spectrometer (Spectrum One, Perkin-Elmer, UK) in the

region of 650–4000 cm^{-1} with a resolution of 4 cm^{-1} and 64 scans per spectrum. A moderate pressure was applied (5 psi) to establish good contact between the specimen and the ATR surface [30, 31].

2.3 Dentin Specimen Preparation and Bonding Procedures

Thirty smear-layer covered middle-dentin specimens obtained from additional sound human third molars were prepared as previously described. After acid-etching (37% H_3PO_4; 15 s) the specimens were pre-treated by immersion in deionized water (DW) (n^o sp. =10) or were immersed in one of the two biomimetic primer solutions tested in this study: (i) PLA (n=10); (ii) TMP+PLA (n=10). Subsequently, these specimens were washed with DW (5 s) air-dried (3s) and immediately primed using two consecutive layers of the adhesive control primer Pr.CTR. Two consecutive layers of the filler-free Res.CTR (n^o sp. =5) or ion-releasing resin (Res.IR) (n^o sp. =5) were applied and light-cured for 30s using a Translux EC halogen light-curing unit (KulzerGmbH, BereichDental, Wehrheim, Germany) at a distance of 1 (±0.5) mm. The bonding procedures were completed by applying the resin composite (TetricEvo Cerams, Ivoclar Vivadent, Schaan, Liechtenstein) with five 1 mm layer increments and light-cured for 40s. Further details about the bonding procedures are depicted in Figure 1.

2.4 AFM Imaging and Nano-Indentation

The resin bonded-dentin specimens prepared for each group were longitudinally sectioned into multiple 1.5 mm-thick slabs (3 each specimen) and polished through ascending SiC papers from #800 up to #4000- grit. Further final polishing procedure was performed using diamond pastes (Buheler-MetaDi, Buheler Ltd., Lake Bluff, IL, USA) through 1 μm down to 0.25 μm. The specimens were cleaned in ultrasonic bath (Model QS3, Ultrawave Ltd, Cardiff, UK) containing deionized water [pH 7.4] for 5 min at each polishing step.

An atomic force microscope (AFM-Nanoscope V, Digital Instruments, Veeco Metrology group, Santa Barbara, CA, USA) equipped with a Triboscope indentor system (Hysitron Inc., Minneapolis, MN) and

a Berkovich indenter (tip radius ~20 nm) was employed for the imaging and nano-indentation processes in a fully hydrated status as recently described by Sauro *et al.* [25]. Briefly, five indentations with a load of 4000 nN and a time function of 10 s were performed after different AS storage periods (24 h, 30 days, 90 days) in a straight line starting from the top of hybrid layer down to the underlying intertubular dentin in order to evaluate changes in the modulus of elasticity (Ei) of hybrid layers. Three indentation lines 15(±5) μm from each other were made in five different mesio-distal positions along the interface. The apical-occlusal distance between each indentation was kept constant (5 ± 1 μm) by adjusting the distance intervals steps (Figure 1) and the load function [25, 32].

A Kolmogorov–Smirnov test was conducted to assess data distribution ($P>0.05$) and data were analyzed by ANOVA including analysis of interactions ($P<0.05$). Bonding procedure and storage period in AS were considered as independent variables. Student t test ($P<0.001$) and Student–Newman–Keuls ($P<0.05$) were used for post-hoc comparisons.

2.5 Dye-Assisted Confocal Laser Scanning Microscopy Evaluation (micropermeability analysis)

Three acid-etched dentin specimens for each group were bonded as previously described with the tested resin-based systems mixed with 0.2 wt% Rhodamine B (Sigma–Aldrich). After 24 h, all the specimens had their pulp chambers (PCs) exposed and immediately filled with 0.1 wt% sodium fluorescein solution (Sigma–Aldrich) for 3 h. The PCs of the other half part of specimens were immersed in AS for 90 days and only subsequently the PCs were filled with the fluorescein solution; the AS was replaced every 72 h [25, 33].

All the specimens immersed in fluorescein were treated in an ultrasonic bath for 2 min, sectioned into slabs (1.5 mm) and finally polished using a 1200-grit SiC paper for 1 min. A confocal laser scanning microscope (DM-IRE2 CLSM; Leica, Heidelberg, Germany) equipped with a 63×/1.4 NA oil immersion lens and a 488-nm Argon/Krypton (Fluorescein excitation) or 568-nm Helium/Neon ions laser (Rhodamine B excitation) was used to analyze the ultra-morphology and micropermeability along the bonded-dentin interfaces; the emission fluorescence was recorded at 512–538 nm and 585–650 nm, respectively. Reflection and fluorescence optical images were captured 5 μm below

the outer surface up to 25 µm depth (1 µm z-step) and converted in topographic and/or single projections using the Leica SP2 CLSM image-processing software (Leica, Heidelberg, Germany) [34]. The configuration of the system was standardized and used at the same level throughout the entire investigation.

2.6 Qualitative Raman Spectroscopy and Quantitative Cluster Analysis

The same specimens submitted to AFM imaging/nano-indentation were also analyzed using a dispersive Raman spectrometer/microscope (Horiba Scientific Xplora, Villeneuve d'Ascq, France) after 24h and 90 days of AS storage (Fig.1). A 785-nm diode laser (100 mW sample power) equipped with a ×100/0.90 NA water-immersion objective was employed. Raman signals were acquired using a 600-lines/mm grating centered between 900 and 1700 cm^{-1}. Three chemical mappings were captured along the interfaces (two in proximity of the pulpal horns and one in the middle of the pulpal floor) and submitted to K-means cluster (KMC) analysis as described by Toledano *et al.* [33], using multivariate analysis (ISyss Horiba), which includes statistical patterning to derive independent clusters; the biochemical content of each cluster was analyzed using the average cluster spectra. Principal component analysis (PCA) decomposed data were set into a bilinear model of linear independent variables, the so called principal components (PCS). Five to six clusters were identified but only three representative clusters, always present in all the specimens before and after AS storage, were considered and values for each cluster such as demineralized dentin, sound dentin and resin-collagen hybrid zone within the interface were independently obtained. At this point, the Mineral Matrix Ratio (MMR: the ratio of integrated areas of the phosphate P–O symmetric stretch [ν1 - 961 cm^{-1}] and contour of the CH_2 deformation of the collagen [1465 cm^{-1}]) was measured for the same cluster in each group, in order to quantitatively calculate the extent of mineralization along the interface. Data were analyzed by ANOVA and Tukey's post-hoc test for pairwise comparisons ($P<0.05$).

2.7 Micro-Tensile Bond Strength (µTBS) and Fracture Ultra-morphology Analysis (FEG-SEM)

A further five resin-bonded dentin specimens were prepared for each group and sectioned in both X and Y directions to obtain multiple bonded-sticks of 0.9 mm^2. Their microtensile bond strengths were tested after 24 h or 90 days of AS storage using a customized microtensile jig on a linear actuator (SMAC Europe Ltd., Horsham, West Sussex, UK). Mean bond strength values were analyzed by ANOVA, which was performed including the bond strength (MPa) as the dependent variable. Bonding groups (CTR, PLA and TMP+PLA) and period of AS storage (24 h and 90 days) were considered as independent variables. Analysis of interactions was also conducted. Student–Newman–Keuls test was used for multiple comparisons. Statistical analysis was set at a significance level of α=0.05. Modes of failure were classified as percentage of adhesive (A) or mixed (M) or cohesive (C) failures using a stereo microscope (magnification ×60). Three representative fractured specimens for each group were mounted on aluminum stubs using carbon tape, gold sputter coated and finally imaged using FEG-SEM (Gemini, Carl Zeiss, Oberkochen, Germany) at 3 kV and a working distance of 15 mm.

3. RESULTS

3.1 ATR-FTIR Analysis of Dentin Collagen

Dentin before acid-etching presented phosphate bands at 885–1180 cm^{-1} (phosphate stretching mode) representative of mineral components, amide bands from organic components (1200–1725 cm^{-1}) and O–H stretching of water (H_2O) at 3200–3400 cm^{-1} [31, 35]. When dentin was acid-etched, a clear presence of collagen at 1650 cm^{-1} and 1540 cm^{-1} (C=O - amide I and CNH - amide II, respectively) as well as very low intensity peaks at 1083 cm^{-1} and 1034 cm^{-1} identified the loss of the P–OR esters (Figure 2). The application of the biomimetic primers PLA or TMP+PLA biomimetic solutions increased the phosphate peaks at 1083 cm^{-1} and 1034 cm^{-1} and induced the formation a further PO stretching peak at 967 cm^{-1}(*v*3 – asymmetric stretching mode of hydroxyapatite) [29]. The vibrational stretching of the CO–C alcohol group (1048 cm^{-1}) was also evident after biomimetic primer treatments, identifying the presence of HEMA (resin primer) which also showed the C–O–C peak at 1090 cm^{-1} [30].

3.2 AFM Nano-indentation and dye-assisted CLSM imaging

The Young's modulus of elasticity (Ei) of the hybrid layer in the second (HL) and the third (BHL) indentations were influenced by the main effects ($P<0.001$); bonding procedure ($P<0.001$) storage period. Interactions between factors were also significant ($P<0.001$), (Table 1).

The first indentation performed along each resin-dentin interface was localized on the top part of the hybrid layer (Figure 1). There was no significant difference ($p>0.05$) between the Ei values of each bonding procedure at the same indentation position (1st Hybrid Layer). Moreover, the aging periods (30 and 90 days) induced no significant change ($p>0.05$) in any of the tested bonding strategies.

The resin-dentin interface created using the control resin (Res.CTR) showed a significant decrease in the nano-elasticity ($p<0.05$) of the hybrid layer (2nd indentation) both after 30 and 90 days of storage in AS (Table 1); the bottom of the hybrid layer showed no change in terms of nano-elasticity ($p>0.05$). The same resin applied after dentin pre-treatment using the primers containing PLA or PLA+TMP showed no significant change ($p>0.05$) in the Ei values of the 2nd indentation of the hybrid layer only after 30 days of AS storage; these values dropped significantly ($p>0.05$) after 90 days of AS immersion. However, the specimens created with Res.CTR/PLA and Res.CTR/TMP+PLA showed no significant change ($p>0.05$) at the bottom of the hybrid layer both after 30 and 90 days of AS storage.

Conversely, the specimens bonded with the remineralising adhesive containing Ca-Silicate/CaP fillers (Res.IR) showed a significant increase of the nano-elasticity ($p<0.05$) in the middle of the hybrid layer (2nd indentation) and at the bottom of the hybrid layer (3rd indentation) after 30 and 90 days of storage in AS, respectively. The same resin applied after pre-treatment with the biomimetic PLA or PLA+TMP primers induced a significant increase of the Ei of the 2nd indentation and al the bottom of

hybrid layer (3rd indentation) both after 30 and 90 days of AS storage. No significant changes were observed in the underlying mineralized dentin ($p>0.05$) over time.

These changes in the nanoelasticity observed for the middle hybrid layer and the bottom of the hybrid layer in specific resin-dentin interfaces were also supported by the AFM and dye-assisted confocal microscopy imaging. CLSM (Figure 2A) as well as the AFM analysis (Figure 2C) showed a sound gap-free resin-dentin interface in the specimens created with the Res.IR after 90 days. These specimens also showed hybrid layers characterized by an important micropermeability and a clear image of the ion-releasing filler particles (analysis in reflection mode) within the adhesive layer and inside the dentinal tubules. The specimen created with the control resin (Res.CTR) showed a gap-free resin-dentin interface characterized by high micropermeability of the hybrid layer, but with no reflection signal, as there was no fillers in the adhesive layer or inside the dentinal tubules (Figures 2B and 2D).

Several important morphological changes were observed along the resin-dentin interfaces after 90 days of AS storage. For instance, the CLSM imaging performed on the resin-dentin specimens created with the control resin filler-free showed the presence of a gap between the hybrid layer and the underlying dentin; slight micropermeability was only detectable at the bottom of the hybrid layer (Figures 3A and 4A). The resin-dentin interfaces created with the control filler free resin (Res.CTR) applied to the dentin pretreated with the PLA (Figure 3B) or PLA+TMP primers (Figure 3C) were also characterized by a degradation-induced gap within the interface with residual micropermeability at the bottom of the hybrid layer.

Conversely, the resin-dentin interface created with the experimental Res.IR showed no gap between the adhesive and the hybrid layer but a strong reflection signal generated by fillers present within the adhesive layer and the hybrid layer; such specimens showed lower micropermeability (Figure 3D). The integrity of this interface created with the ion-releasing mineralizing adhesive (Res.IR) after prolonged aging was also confirmed by the AFM analysis, which showed the presence of an intact hybrid layer (Figure 4B). However, when the resin-dentin interface created with Res.IR/PLA bonded

specimens was immersed in AS for 90 days, important mineral precipitation was detected within the hybrid layer along with low micropermeability (Figure 3E); no gap was observed within this resin-dentin interface after 90 days of storage (Figure 4C). The same situation was encountered in specimens created with the experimental ion-releasing resin (Res.IR) applied to dentin pretreated with the PLA+TMP-containing biomimetic primer. Indeed only a very week micropermeability signal was detected within the hybrid layer; the hybrid layers appeared crystallized/remineralized both when analyzed with the dye-assisted CLSM (Figure 3E) and AFM (Figure 4D).

3.3 Qualitative Raman Spectroscopy and Quantitative Cluster Analysis

Three main clusters were considered in this test as being constantly present and quantitatively analyzable in all the specimens before and after prolonged AS storage (24h and 90 days): (i) sound dentin; (ii) demineralized dentin; and (iii) resin-collagen hybrid zone (Figures 5A to 5D). A typical Raman spectrum was obtained in the regions of 900–1200 cm^{-1} and 1200–1800 cm^{-1} for the sound/untreated dentin (Figure 5A). The intense peaks at 961 cm^{-1} and 1010 cm^{-1} are respectively associated with the phosphates (PO_4^{3-} $\nu 1$) and (PO_4^{3-} $\nu 3$), while the peak at 1073 cm^{-1} represents the carbonates (CO_3^{2-} $\nu 1$) of the dentin apatite. The bands at 1245, 1452, and 1667 cm^{-1} are attributed to the organic components of collagen, CH_2 vibrations, and type I collagen (C=O), respectively [36]. The same peaks were clearly identified in the spectra of the demineralized dentin, although the phosphate peak at 961 cm^{-1} gave a much lower result when compared to mineralized dentin (Figure 5B). The cluster comparison of the resin-collagen hybrid zones attained in the specimens created with the filler-free control resin (Res.CTR) or the ion-releasing resin (Res.IR) with or without the biomimetic pre-treatment primers (PLA and TMP+PLA) presented slight chemical differences. Indeed, the hybrid zone created with the Res.CTR was similar to the cluster spectra of the demineralized dentin (Figure 5C), even though characterized by aromatic and aliphatic components of the resin-based system at 1608 and 1638 cm^{-1} [37, 38]. Conversely, the hybrid zone created using the Res.IR differed from that of Res.CTR for the presence of the crystalline carbonates at 1100 cm^{-1} (CO_3^{2-} $\nu 2$) and calcium silicates at 1529 and 1770 cm^{-1} (Figure 5D) within the demineralized collagen

[39]. The MMR measurements of the ratio of the phosphate P–O symmetric stretch (961 cm^{-1}) to that of collagen (1465 cm^{-1}) for the same cluster in each group (Figures 5E and 5F) showed that after 90 days of AS storage, only specimens bonded with the ion-releasing rein (Res.IR) was able to produce a significant increase ($p<0.05$) in remineralization at the resin-dentin interface both when applied with or without use of biomimetic primers PLA or TMP+PLA. However, the highest level of remineralization ($p<0.05$) of the hybrid zone at the resin-dentin interface was obtained only when the ion-releasing resin (Res.IR) was used in conjunction with the biomimetic primer TMP+PLA bonding procedure was employed. This was also evident when the MMR measurements of the specimens bonded using the Res.IR/PLA+TMP or Res.IR/PLA were converted into topographic images (Figure 5G to 5L). Indeed, the Res.IR/PLA+TMP showed a noticeable gradient of mineralization both at the underlying dentin and along the bonded interface, although very few parts of the hybrid zone presented low remineralization probably due to higher resin infiltration (Figure 5H). The specimens created using the Res.IR/PLA (Figure 5L) showed remineralization at the underlying dentin (d), but with a lower gradient of mineralization along the bonding interface (i.e. hybrid zone) when compared to the specimens created with the Res.IR/PLA+TMP bonding procedure.

3.4 Micro-Tensile Bond Strength (μTBS) and Fracture Ultra-morphology Analysis (FEG-SEM)

Bond strength was affected by bonding procedures ($F=7.57$; $P<0.001$) and storage time ($F=165.12$; $P<0.01$). Interactions were also significant ($F=7.23$; $P<0.001$). The power of the ANOVA was 0.72. Mean bond strength values obtained for each experimental group are summarized in Table 2.

The bond strength (μTBS) of the filler-free control resin (Res.CTR) applied on acid-etched dentin was 39.5 (±4.8) MPa after 24 h of AS storage, with the specimens debonded specimens exhibiting primarily mixed failures (85%). However, a significant drop ($p < 0.05$) in the μTBS of the control resin bond values (26.8 ±3.8) was observed after 90 days of AS storage, along with an increase in the number of adhesive fails (40%). The SEM-FEG ultra-morphology analysis performed on the these debonded control specimens (Res.CTR) at 24h of AS storage showed some remnant resin, the presence of dentinal tubules prevalently occluded by resin tags (Figure 6A) and remnant collagen

fibrils not completely resin infiltrated (Figure 6B). However, after 90 days of storage, the same specimens showed a failure ultra-morphology characterized by intertubular and intratubular dentin free of fibrils and no mineral precipitation; some fractured resin tags were still present inside the dentin tubules (Figure 7A). Likewise, the filler-free resin (Res.CTR) applied on acid-etched dentin pre-treated with PLA or TMP+PLA showed at 24 h of AS storage bond strength values of 41.2 (±3.8) and 36.0 (±6.3) respectively. After 90 days of AS storage, specimens treated with either biomimetic primers showed significantly lower μTBS values ($p<0.05$), [Res.CTR/PLA: 25.9 (±5.8); Res.CTR/TMP+PLA: 19.3 (±3.4)] and the number of adhesive fails increased up to 65% for the specimens in the group Res.TMP+PLA. The SEM-FEG ultra-morphology analysis showed dentinal tubules partially and/or completely occluded by resin tags as well as remnant resin on the dentin surface (Figures 6C and 6E). However, at higher magnification, the specimens bonded with Res.CTR/PLA showed very few remnant collagen fibrils (Figure 6D), while those created with the Res.CTR/TMP+PLA were characterized by an important presence of intact collagen fibrils (Figure 6F). After 90 days of AS storage, both groups bonded with biomimetic primers and control resins debonded leaving behind dentin surfaces devoid of clear mineral precipitation within the few collagen fibrils remained on the dentin surfaces (Figures 7B and 7C). The specimens bonded with the ion-releasing resin (Res.IR), their 24h μTBS were 35.3 (±5.9) MPa, whilst when this resin was applied on acid-etched dentin pre-treated with the PLA or TMP+PLA the μTBS was 37.1 (±5.2) and 31.4 (±4.6) MPa, respectively. No significant difference ($p>0.05$) was observed between the bonding procedures tested in this study at 24h of AS storage.

The SEM ultra-morphology analysis of the Res.IR specimens debonded after 24h of AS storage showed a surface with residual resin (Figure 6G) and fractured resin tags inside dentinal tubules; collagen fibrils were detected on the dentin surface (Figure 6H). The resin Res.IR/PLA debonded in the mixed mode, leaving a fractured surface covered by residual resin; this latter was characterized by several voids created by the loss of ion-releasing filler particles (Figures 6I and 6L). In the case of the specimens created with the resin Res.IR/TMP+PLA, it was possible to detect after debonding a

surface mainly covered by the resin (Figure 6M) with several voids created by the loss of filler particles (Figure 6N). However, when these specimens were tested after 90 days of AS storage, only those specimens bonded with Res.IR/TMP+PLA showed no significant drop in the bond strength values ($p>0.05$) and most specimens debonded prevalently in the mixed (85%) mode. Conversely, the μTBS values of the specimens in the Res.IR and Res.IR/PLA groups fell significantly ($p<0.05$) (Table 2) after 90 days of storage and the number of failures in adhesive mode increased to 35% for the Res.IR and 30% for the Res.IR/PLA compared to those attained after 24h of AS storage. The ultra-morphology of the debonded specimens created with the resin Res.IR was characterized by several exposed resin tags which were totally covered by minerals (Figure 7D and 7E); the same morphology was observed for the specimens in the group Res.IR/PAL (Figure 7G). This mineral precipitation was also evident in dentin surfaces which presented no clear presence of exposed collagen, both for the specimens created with the Res.IR (Figure 7E) and Res.IR/PLA (Figures 7H and 7I).

The ultra-morphology of the debonded specimens of the group Res.IR/TMP+PAL was characterized by a surface, that was clearly mineralized and resin tags still inside the dentinal tubules (Figure 7L). At higher magnification (Figure 7M) this remineralization was clearer as the dentin surface appeared devoid of exposed collagen fibrils and covered by mineral crystals; indeed, nano-crystal deposition was evidently observed on the collagen fibrils in the intertubular dentin (Figure 7N).

4. DISCUSSION

Reliable, functional remineralization of acid-etched resin-bonded dentin interface as well as those created in caries-affected dentin, should be able to induce intra-fibrillar and extra-fibrillar mineral deposition with hydroxyapatite (HA) crystals orientated in the same direction as those in sound dentin [40]. This should result in re-establishment of the modulus of elasticity of mineral-depleted dental structures within bonding interfaces [21, 27, 41]. It has been demonstrated that mineral-depleted collagen previously infiltrated with amorphous biomimetic precursors can be properly remineralized by direct crystallization processes [40, 42].

The present study has shown how an experimental light-curable resin-based system containing Ca-silicate/CaP-releasing micro-fillers may remineralize mineral-depleted resin-dentin interfaces once applied on acid-etched dentin pre-treated with biomimetic primers containing polyanionic compounds such as sodium trimetaphosphate (TMP) and/or polyaspartic acid (PLA). Thus, the null hypothesis that the pre-treatment of demineralized dentin with biomimetic analogues does not improve the remineralization ability of light-curable resin-based systems doped with ion-releasing micro-fillers at the mineral-depleted resin–dentin interface must be partially rejected.

The FTIR-ATR results obtained in this study showed that the pre-treatment of acid-etched dentin with PLA or TMP+PLA biomimetic primers induced phosphate uptake in demineralized dentin collagen [30] with an increase of the peaks at 1083 cm^{-1} and 1034 cm^{-1} and with the formation of the PO asymmetric stretching mode of hydroxyapatite at 967 cm^{-1} (Figure 2). As previously mentioned [40, 42], this feature should be considered as the main key factor for the bio-remineralization of the resin-dentin interfaces. Indeed, those resin-dentin interfaces created with the Res.IR applied onto an acid-etched dentin pre-treated with the PLA or TMP+PLA primers showed significantly higher Ei values at the resin-dentin interface when compared to those attained with the Res.IR alone. This was particularly evident when the Res.IR was used in combination with the biomimetic primer TMP+PLA as this bonding procedure was able to reestablish a significantly higher modulus of elasticity at the 2^{nd} hybrid layer and bottom of the hybrid layer both after 30 and 90 days of AS storage (Table 1). Restoration of the mechanical properties of the hybrid layer was evaluated using nano-indentations performed on the hydrated tissue. The changes in nano-elasticity (Ei) observed for the middle and the bottom of the hybrid layer when using the experimental ion-releasing resin (Res.IR) in combination with the two tested biomimetic primers were also supported by the AFM and dye-assisted CLSM analysis; this latter showed the presence of a strong reflection signals generated by the mineral deposits within the hybrid layer that where associated with reduced micropermeability (Figure 3D) of those hybrid layers. There was integrity of the bonded interface created with the Res.IR and the presence of an intact hybrid layer after prolonged AS aging (Figure 4B), rather than

the gap seen in resin-dentin interfaces created with the control resin (Res.CTR) (Figure 3A and 4A), that may be due to collagen degradation by endogenous dentin proteases as previously reported in several scientific publications [8, 13, 18, 24, 29]. Conversely, the pre-treatment of acid-etched dentin using the two biomimetic primers, but in particular with the use of the TMP+PLA, favored a consistent mineral deposition that reduced the micropermeability of hybrid layers to a minimum level. Indeed, the resin-dentin interface created with the Res.IR/TMP+PLA appeared extensively remineralized (Figure 3E and 4D). Moreover, quantitatively Raman MMR measurements of phosphate P–O (961 cm^{-1}) symmetric stretch and collagen (1465 cm^{-1}) subsequent to the cluster analysis (Figures 5E and 5F) showed that only Res.IR was able to induce a significant increase ($p<0.05$) in remineralization of the resin-dentin interface after 90 days of AS storage, both when applied with or without the two tested biomimetic primers. The highest level of remineralization ($p<0.05$) of the hybrid zone at the resin-dentin interface was obtained when using the combination of Res.IR/TMP+PLA bonding. The remaining presence of some areas with lower remineralization (Figure 5H) is thought to be due to areas where resin infiltrated the demineralized matrix, which impaired the mineral deposition within the dentin collagen at the hybrid layer [21]. These results are in accordance with previous studies [14, 21, 40] where a similar approach based on a phosphate-free, calcium-silicate Portland cement, and a phosphate-containing fluid system was used in the presence of polyacrylic acid as stabilizer for amorphous calcium phosphates and polyvinylphosphonic acid (PVPA) as a collagen-binding matrix protein to evoke extra-fibrillar and intra-fibrillar bio-remineralization of acid-etched dentin collagen within hybrid layers. Water-saturated, uninfiltrated collage fibrils are commonly susceptible to degradation due to hydrolytic instability and/or enzymatic activity.

Pure Portland-based cements may contain potential cytotoxic agents due to the high alkaline (pH: 12) and to the presence of arsenic ions. Therefore, these cements are not suitable for clinical application because they also lack of radiopacity [43, 44]. Nevertheless, these types of cements, commonly known as Mineral Trioxide Aggregate (MTA), have found important applications in

dentistry due to their bioactive remineralization properties [45, 46]. For instance, MTA cements can be used in atraumatic restorative treatments (ART) as indirect pulp capping materials after minimal cavity preparation in deep caries lesions. However, this approach requires the presence of phosphate-containing body fluids in order to evoke a proper remineralization of the mineral-depleted dentin [47]. It has recently been reported that a biomimetic mineralization of caries-like lesions is possible when using Portland cements in the presence of a simulated body fluid containing polyacrylic acid and polyvinylphosphonic acid/sodium tripolyphosphate [20, 48]. Although this technique achieves an effective remineralization *in vitro*, it cannot be adopted clinically to remineralize carious-affected dentin and /or mineral-depleted interfaces as the biomimetic analogs cannot be dissolved in body fluids. The results of the present study demonstrated how an alternative approaches based on the pre-treatment of demineralized dentin with aqueous biomimetic primers and PLA and/or TMP may be used as a valid remineralization strategy.

The main difference between the biomimetic remineralization strategy for clinical application proposed by Liu *et al*. [48] and that proposed in this study is the use of the polyaspartic acid instead of the polyacrylic acid as the stabilizer for amorphous calcium phosphates. Both polyaspartic and polyacrylic acids act as biomimetic analogs of matrix proteins which participate in the recruitment of pre-nucleation clusters to produce fluidic, polymer-stabilized amorphous calcium phosphate nano-precursors [47-49]. Gower *et al.* [50] postulated that the formation of liquid nano-precursors sequestered by polyanionic polymers may be a fundamental step in biomineralization [45]. Indeed, these fluidic nano-precursors infiltrate collagen fibrils and transform into intra-fibrillar apatite using the fibrils as bio-mineralization templates [48, 43]. This study is in accordance with the results of Burwel *et al.* [27] who showed that using PLA as the polymer-induced liquid-precursor, it is possible to gradually recover the mineral content and also recover substantial mechanical properties of artificial caries lesions; that vary with location in the lesion, and included full recovery in the deeper portions and less recovery in the more demineralized portions. On the contrary, in the absence of polyaspartic acid, shallower artificial lesions showed very little improvement in their mechanical

properties, and often areas of mineral precipitation were apparent. Indeed, the present study showed that the resin-dentin interface created with Res.IR only gradually reached full recovery in the deeper portion of the interface (bottom of the hybrid layer), with less recovery of the modulus of elasticity in the more demineralized portion of hybrid layers. The hybrid layer created with the Res.IR applied on the acid-etched dentin pre-treated with the TMP+PLA primer showed practically complete recovery of the modulus of elasticity of the dentin (Table 1). The presence of remnant apatite seed crystallites at the bottom of the hybrid layer or in caries affected dentin can act as centers for heterogeneous nucleation creating a situation thermodynamically more favorable than homogeneous epitaxial nucleation (top–down remineralization approach) within a completely demineralized and/or resin-infiltrated collagen matrix [51]. Conversely, the remineralization of hybrid layers created with the Res.IR/TMP+PLA may have occurred due to a bottom–up process based on the non-classical theory of crystallization, which involves the use of the biomimetic analogs which generated metastable amorphous mineral precursors and mesocrystals that infiltrate and remineralize the intra-fibrillar portion of the collagen fibrils; this latter was presumed to be responsible for restoring the mechanical properties of dentin [52]

A high quality and durable hybrid layer can be only achieved if the demineralized dentin collagen fibrils within the resin-dentin interface are fully resin-encapsulated during bonding procedures. Evidence of degradation has been extensively reported [15, 18, 55] for “poorly” resin-infiltrated hybrid layer and at its bottom, in particular in bonds made with etch-and-rinse systems. Such hybrid layers contain more residual water than do self-etching adhesives, making them more susceptible to the proteolytic activity of MMPs [49]. Moreover, the elution of uncured resin monomers along with the hydrolytic polymer degradation may make the situation even worse by increasing the collagenolytic activity of MMPs within resin-dentin interface [23]. Although several methods such as inhibition of the MMPs [56] and collagen cross-linking [57] have been shown to reduce the degradation of the hybrid layer, the bio-remineralization of mineral-depleted resin–sparse regions of the demineralized collagen matrix within the hybrid layer seems to be one of the most suitable

strategies to restore the mechanical properties as well as increase the longevity of the resin–dentin interfaces [21, 23, 26].

The results of this study showed that acid-etched dentin bonded with the control resin (Res.CTR) with or without the pre-treatment with the biomimetic PLA or TMP+PLA primers exhibited significant decrease in μTBS values ($p < 0.05$) after 90 days of AS storage along with an increase in the number of adhesive failures. The SEM-FEG ultra-morphology analysis performed on these debonded specimens showed after 90 days of AS, few remnant collagen fibrils and no mineral precipitation were seen in resin-bonded specimens created with the Res.CTR (Figure 7A), while those created with the Res.CTR/PLA (Figure 6D) or Res.CTR/TMP+PLA (Figure 7B and 7C) showed very few remnant collagen fibrils. Similarly, the specimens created with Res.IR and Res.IR/PLA fall significantly ($p<0.05$) after 90 days of AS and the number of failures in adhesive mode increased to 35% and 30% respectively. The ultra-morphology of the debonded specimens created with these two bonding approaches presented mineral precipitation with no clear presence of exposed collagen (Res.IR, Figure 7E) (Res.IR/PLA, Figure 7H and 7I). These results are in accordance with those presented in previous studies [23, 25, 58] that reported an reduction of the μTBS after 3 months of PBS storage as well as those reported by other studies using glass ionomer cements (GICs) as therapeutic agents for restoration of demineralized dentin [59]. Indeed, the GIC-bonded interfaces may achieve tensile bond strength of 5 MPa with frequent bond failures during sample preparation. Such failures occurred also in the specimens tested in the present study due to a clear mineral precipitation which replaced hydrophilic components (i.e. water and/or HEMA) making the resin-dentin interface (i.e hybrid layer) quite brittle with a high modulus of elasticity (Table 1); thus, under elastic deformation the interface cannot withstand the stress created during microtensile tests. In the present study the remineralized de-bonded interface might have similar mechanical characteristics as those created by GIC when submitted to microtensile tests. [60] Wang *et al.,* [58], stated that more efforts need to be undertaken to further improve the bond strength to dental hard tissues without weakening the demineralization properties. This study has demonstrated that with

the pre-treatment of acid-etched dentin using a biomimetic primers containing polyaspartic acid and/or sodium trimetaphosphate, resin-based systems doped with ion-releasing fillers can be applied as a suitable strategy to restore the mechanical properties as well as increase the longevity of the resin–dentin interfaces. Indeed, the current study showed that specimens created with the Res.IR/TMP-PAL approach had no significant reduction of the μTBS values ($p>0.05$) over 90 days of As storage, unlike the controls. Moreover, these specimens presented a debonded surface devoid of exposed collagen fibrils as they were clearly covered by nano-crystals deposition both in the intertubular and intratubular dentin (Figure 7N).

It may be hypothesized that the use of the biomimetic primers containing TMP and PAL in conjunction with the Ca-silicate/CaP resin induced remineralization by driving the Ca/P deposition mainly within the demineralized collagen fibrils within the hybrid layer (bottom-up remineralization) rather than depositing minerals on the dentin surface (top-down mineralization) [40, 49]. Mismatches in multilayered adhesive assemblies can cause localized stress concentration that can lead to adhesive failure. With more mineral deposition within the hybrid layer, the resin-dentin interface acquires a modulus of elasticity quite similar to that of sound dentin rather than that created with the Res.IR or Res.IR/PLA (Table 1).

5. Conclusion

The results of this study indicate that biomimetic remineralization of resin-bonded dentin is possible within 90 days *in vitro*. The combination of 40wt% Calcium silicate/CaP fillers in a light-curable etch-and-rinse adhesive can remineralize any water-filled voids at the bonded interface and recover the modulus of elasticity of hybrid layers in the presence of artificial saliva (AS), if the acid-etched dentin is pre-treated with biomimetic primers such as poly-L-aspartic acid (PLA) and/or sodium trimetaphosphate (TMP).

6. REFERENCES

1. Marshall GW, Inai N, Wu-Magidi IC, Balooch M, Kinney JH, Tagami J, et al. Dentin demineralization: effects of dentin depth, pH and different acids. Dent Mater, 1997;13:338–343.
2. Murdoch-Kinch CA, McLean ME. Minimally invasive dentistry. J Am Dent Assoc, 2003;134:87-95.
3. Yamaga R, Nishino M, Yoshida S, Yokomizo I. Diammine silver fluoride and its clinical application. J Osaka Univ Dent Sch, 1972;12:1-20
4. Sonoda H, Banerjee A, Sherriff M, Tagami J, Watson TF. An in vitro investigation of microtensile bond strengths of two dentin adhesives to caries-affected dentin. J Dent, 2005;33:335–42.
5. Sauro S, Watson TF, Thompson I, Banerjee A. One-bottle self-etching adhesives applied to dentin air-abraded using bioactive glasses containing polyacrylic acid: an in vitro microtensile bond strength and confocal microscopy study. J Dent, 2012; 40: 896-905.
6. Lynch CD, Blum IR, Frazier KB, Haisch LD, Wilson NH. Repair or replacement of defective direct resin-based composite restorations: contemporary teaching in U.S. and Canadian dental schools. J Am Dent Assoc, 2012; 143:157–163.
7. Jandt KD, Sigusch BW. Future perspectives of resin-based dental materials. Dent Mater, 2009;25:1001–1006
8. Tjäderhane L, Nascimento FD, Breschi L, Mazzoni A, Tersariol IL, Geraldeli S, et al. Strategies to prevent hydrolytic degradation of the hybrid layer-A review. Dent Mater, 2013;29:999-1011.
9. Brackett MG, Li N, Brackett WW, Sword RJ, Qi YP, Niu LN, Pucci CR, et al. The critical barrier to progress in dentin bonding with the etch-and-rinse techniques. J Dent, 2011;39:238-248.
10. Liu Y, Tjaderhane L, Breschi L, Mazzoni A, Li N, Mao J, et al. Limitations in bonding to dentin and experimental strategies to prevent bond degradation. J Dent Res, 2011;90:953-968.

11. Wood JD, Sobolewski P, Thakur V, Arola D, Nazari A, Tay FR, et al. Measurement of microstrains across loaded resin-dentin interfaces using microscopic moiré interferometry. Dent Mater, 2008;24:859-66.
12. Magne D, Weiss P, Bouler JM, Laboux O, Daculsi G. Study of the maturation of the organic (type I collagen) and mineral (nonstoichiometric apatite) constituents of a calcified tissue (dentin) as a function of location: a Fourier transform infrared microspectroscopic investigation. Magne D, Weiss P, Bouler JM, Laboux O, Daculsi G. Journal of Bone and Mineral Research, 2001;16:750-757.
13. Kim YK, Mai S, Mazzoni A, Liu Y, Tezvergil-Mutuay A, Zhang K, et al. Biomimetic remineralization as a progressive dehydration mechanism of collagen matrices – implications in the aging of resin-dentin bonds. Acta Biomaterialia, 2010;6:3729-3739.
14. Qi YP, Li N, Niu LN, Primus CM, Ling JQ, Pashley DH, et al. Remineralization of artificial dental carious lesions by biomimetically modified mineral trioxide aggregate. Acta Biomaterialia 2012;8:836-842.
15. De Munck J, Van Landuyt K, Peumans M, Poitevin A, Lambrechts P, Braem M, Van Meerbeek B. A critical review of the durability of adhesion to tooth tissue: methods and results J Dent Res, 2005;84:118–132.
16. Yiu CK, Tay FR, King NM, Pashley DH, Sidhu SK, et al. Interaction of glass-ionomer cements with moist dentin. J Dent Res, 2004; 83: 283–289.
17. Xie D, Zhao J, Weng Y, Park JG, Jiang H, Platt JA. Bioactive glass-ionomer cement with potential therapeutic function to dentin capping mineralization. Eur J Oral Sci, 2008; 116: 479– 487.
18. De Munck J, Van Meerbeek B, Yoshida Y, Inoue S, Suzuki K, Lambrechts P. Four-year water degradation of a resin-modified glass-ionomer adhesive bonded to dentin. Eur J Oral Sci, 2004; 112: 73–83.
19. Kim YK, Yiu CK, Kim JR, Gu L, Kim SK, Weller RN, et al. Failure of a glass ionomer to remineralise apatite-depleted dentin. J Dent Res, 2010; 89: 230–235.

20. Gu LS, Kim J, Kim YK, Liu Y, Dickens SH, Pashley DH, et al. A chemical phosphorylation-inspired design for Type I collagen biomimetic remineralization. Dent Mater, 2010;26:1077-89.
21. Ryou H, Niu LN, Dai L, Pucci CR, Arola DD, Pashley DH, et al. Effect of biomimetic remineralization on the dynamic nanomechanical properties of dentin hybrid layers. J Dent Res 2011;90:1122–1128.
22. Vollenweider M, Brunner TJ, Knecht S, Grass RN, Zehnder M, Imfeld T, et al. Remineralization of human dentin using ultrafine bioactive glass particles. Acta Biomater, 2007;3:936–943.
23. Profeta AC, Mannocci F, Foxton RM, Thompson I, Watson TF, Sauro S. Bioactive effects of a calcium/sodium phosphosilicate on the resin-dentin interface: A microtensile bond strength, scanning electron microscopy, and confocal microscopy study. Eur J Oral Sci, 2012;120:353–362.
24. Osorio R, Yamauti M, Sauro S, Watson TF, Toledano M. Experimental resin cements containing bioactive fillers reduce matrix metalloproteinase–mediated dentin collagen degradation. J, Endod, 2012;38:1227–1232.
25. Sauro S, Osorio R, Watson TF, Toledano M. Therapeutic effects of novel resin bonding systems containing bioactive glasses on mineral-depleted areas within the bonded-dentin interface. J Mater Sci: Mater Med, 2012;23:1521–1532.
26. Liu Y, Mai S, Li N, Yiu CK, Mao J, Pashley DH, et al. Differences between top-down and bottom up approaches in mineralizing thick, partially demineralized collagen scaffolds. Acta Biomater, 2011; 7:1742–1751
27. Burwell AK, Thula-Mata T, Gower LB, Habelitz S, Kurylo M, Ho SP, et al. Functional remineralization of dentin lesions using polymer-induced liquid-precursor process. PLoS One, 2012; 7:e38852.
28. Deshpande AS, Beniash E. Bioinspired synthesis of mineralized collagen fibrils. Crystal Growth Design, 2008;8:3084–90.
29. Tezvergil-Mutluay A, Seseogullari-Dirihan R, Feitosa PV, Tay FR, Watson TF, Pashley DH, et al. Zoledronate and Ion-releasing Resins Impair Dentin Collagen Degradation, J Dent Res, 2014;93:999-1004.

30. Sauro S, Osorio R, Fulgêncio R, Watson TF, Cama G, Thompson I, et al. Remineralisation properties of innovative light-curable resin-based dental materials containing bioactive micro-fillers J Mater Chem B, 2013; 1: 2624-2638
31. Feitosa VP, Bazzocchi MG, Putignano A, Orsini G, Luzi AL, Sinhoreti MA, et al. Dicalcium phosphate (CaHPO4·2H2O) precipitation through ortho- or meta-phosphoric acid-etching: effects on the durability and nanoleakage/ultra-morphology of resin-dentin interfaces. J Dent, 2013;41:1068-1080.
32. Toledano M, Sauro S, Cabello I, Watson T, Osorio R. A Zn-doped etch-and-rinse adhesive may improve the mechanical properties and the integrity at the bonded-dentin interface. Dent Mater, 2013;29:e142-52.
33. Toledano M, Aguilera FS, Sauro S, Cabello I, Osorio E, Osorio R. Load cycling enhances bioactivity at the resin-dentin interface. Dent Mater. 2014;30:e169-188
34. Sauro S, Watson TF, Thompson I, Toledano M, Nucci C, Banerjee A. Influence of air-abrasion executed with polyacrylic acid-Bioglass 45S5 on the bonding performance of a resin-modified glass ionomer cement. Eur J Oral Sci 2012;120:168–77.
35. Bachmann L, Diebolder R, Hibst R, Zezell DM. Changes in chemical composition and collagen structure of dentine tissue after erbium laser irradiation. Spectrochim Acta A Mol Biomol Spectrosc, 2005;61:2634-2639.
36. Penel G, Leroy G, Rey C, Bres E. MicroRaman spectral study of the PO4 and CO3 vibrational modes in synthetic and biological apatites. Calcif Tissue Int, 1998;63:475-481
37. Wang Y, Spencer P Analysis of acid-treated dentin smear debris and smear layers using confocal Raman microspectroscopy. J Biomed Mater Res, 2002;60:300-308.
38. Leung Y, Morris MD. Characterization of the chemical interactions between 4-META and enamel by Raman spectroscopy. Dent Mater, 1995; 11: 191–195
39. Genge MJ, Jones AP, Price GD. An infrared and Raman study of carbonate glasses: Implications for the structure of carbonatite magmas. Geo et Cosm Acta, 1995; 59: 927-937.

40. Tay FR, Pashley DH. Guided tissue remineralisation of partially demineralised human dentine. Biomaterials 2008; 29: 1127-1137.
41. Bertassoni LE, Habelitz S, Marshall SJ, Marshall GW. Mechanical recovery of dentin following remineralization in vitro–an indentation study. J Biomech, 2011;44: 176-181.
42. Nudelman F, Pieterse K, George A, Bomans PH, Friedrich H, et al. The role of collagen in bone apatite formation in the presence of hydroxyapatite nucleation inhibitors. Nat Mater, 2010; 9: 1004-1009.
43. Tenório de Franca TR, da Silva RJ, Sedycias de Queiroz M, Aguiar CM. Arsenic content in Portland cement: a literature review. Indian J Dent Res, 2010; 21:591–595.
44. Torabinejad M, Parirokh M. Mineral trioxide aggregate: a comprehensive literature review--part II: leakage and biocompatibility investigations. J Endod, 2010; 36:190–202.
45. Camilleri J, Pitt Ford TR. Mineral trioxide aggregate: a review of the constituents and biological properties of the material. Int Endod J, 2006; 39:747–754.
46. Parirokh M, Torabinejad M. Mineral trioxide aggregate: a comprehensive literature review--Part I: chemical, physical, and antibacterial properties. J Endod, 2010;36:16–27.
47. Yi-pin Qi, Nan Li N, Niu L, Primus CM, Ling J, Pashley DH, et al. Remineralization of artificial dentinal caries lesions by biomimetically modified Mineral Trioxide Aggregate. Acta Biomater, 2012; 8: 836–842.
48. Liu Y, Li N, Qi Y, Niu LN, Elshafiy S, Mao J, et al. The use of sodium trimetaphosphate as a biomimetic analog of matrix phosphoproteins for remineralization of artificial caries-like dentin. Dent Mater, 2011; 27:465–477.
49. Niu LN, Zhang W, Pashley DH, Breschi L, Mao J, Chen JH, et al. Biomimetic remineralization of dentin. Dent Mater, 2014;30:77-96.
50. Gower LB. Biomimetic model systems for investigating the amorphous precursor pathway and its role in biomineralization. Chem Rev, 2008; 108: 4551-4627.
51. Kim YY, Douglas EP, Gower LB. Patterning inorganic (CaCO3) thin films via a polymer-induced liquid-precursor process. Langmuir. 2007;23:4862-70.

52. Gajjeraman S, Narayanan K, Hao J, Qin C, George A. Matrix macromolecules in hard tissues control the nucleation and hierarchical assembly of hydroxyapatite. J Biol Chem, 2007;282:1193–204.
53. Bertassoni LE, Habelitz S, Kinney JH, Marshall SJ, Marshall Jr GW. Biomechanical perspective on the remineralization of dentin. Caries Res, 2009;43:70–7.
54. Spencer P, Ye Q, Park J, Topp EM, Misra A, Marangos O, et al. Adhesive/Dentin interface: the weak link in the composite restoration. Ann Biomed Eng, 2010;38:1989–2003.
55. Sauro S, Osorio R, Watson TF, Toledano M. Assessment of the quality of resin-dentin bonded interfaces: an AFM nano-indentation, μTBS and confocal ultramorphology study. Dent Mater. 2012;28:622-31
56. Almahdy A1, Koller G, Sauro S, Bartsch JW, Sherriff M, Watson et al. Effects of MMP inhibitors incorporated within dental adhesives. J Dent Res. 2012;91:605-11.
57. Bedran-Russo AK, Pauli GF, Chen SN, McAlpine J, Castellan CS, Phansalkar RS, et al. Dentin biomodification: strategies, renewable resources and clinical applications. Dent Mater, 2014;30:62-76.
58. Wang Z, Shen Y, Haapasalo M, Wang J, Jiang T, Wang Y, et al. Polycarboxylated microfillers incorporated into light-curable resin-based dental adhesives evoke remineralization at the mineral-depleted dentin. J Biomater Sci Polym Ed, 2014;25:679-697.
59. Yip HK, Tay FR, Ngo HC, Smales RJ, Pashley DH. Bonding of contemporary glass ionomer cements to dentin. Dent Mater, 2001;17:456–470.
60. Hewlett ER, Caputo AA, Wrobel DC. Glass ionomer bond strength and treatment of dentin with polyacrylic acid. J Prosthet Dent, 1991;66:767–772.

Table 1: Mean (GPa) and standard deviation (±SD) of Young's modulus of elasticity (Ei) measured along the experimental resin–dentin interfaces.

Ei	24h	30 days	90 days	Interactions (F and P)
Res.CTR				**1st Hybrid layer**
1st Hybrid layer	**3.2±0.8 [Aa]**	**3.1±0.9 [Aa]**	**2.4±0.8 [Aa]**	Main effects: F= 13.05; P= 0.09
2nd Hybrid layer	**1.3±0.3 [Aa]**	**0.8±0.2 [Ba]**	**0.2±0.3 [Ca]**	Bonding type: F= 5.04; P= 0.03
3rd Bottom hybrid layer	**8.5±1.2 [Aa]**	**8.4±1.2 [Aa]**	**8.8±1.1 [Aa]**	Aging: F= 9.18; P= 0.068
4th Underlying dentin	**17.7±2.1 [Aa]**	**17.8±1.9 [Aa]**	**17.9±1.4 [Aa]**	Interactions: F= 2.36; P= 0.88
5th Underlying dentin	**19.5±1.3 [Aa]**	**19.4±1.2 [Aa]**	**19.6± 1.1 [Aa]**	
Res.PLA				
1st Hybrid layer	**3.1±1.0 [Aa]**	**3.1±1.1 [Aa]**	**2.8±1.2 1 [Aa]**	**2nd Hybrid layer**
2nd Hybrid layer	**1.2±0.5 [Aa]**	**0.9±0.2 [Ba]**	**0.3±0.2 [Ca]**	Main effects: F= 19.05; P <0.001
3rd Bottom hybrid layer	**9.8±1.3 [Aa]**	**9.9±1.3 [Aa]**	**10.1±1.5 [Ab]**	Bonding type: F= 29.04; P <0.001
4th Underlying dentin	**17.6±2.1 [Aa]**	**17.5±1.9 [Aa]**	**18.1±1.4 [Aa]**	Aging: F= 5.16; P<0.001
5th Underlying dentin	**18.9±1.3 [Aa]**	**19.3±1.2 [Aa]**	**19.4± 1.1 [Aa]**	Interactions: F= 0.36; P < 0.001
Res.TMP+PLA				
1st Hybrid layer	**3.0±1.1 [Aa]**	**2.9±1.2 [Aa]**	**2.9±1.5 [Aa]**	
2nd Hybrid layer	**1.4±0.6 [Aa]**	**1.0±0.3 [Ba]**	**0.4±0.4 [Ca]**	**3rd Bottom hybrid layer**
3rd Bottom hybrid layer	**9.7±1.4 [Aa]**	**9.8±1.3 [Aa]**	**10.3±1.2 [Ab]**	Main effects: F= 25.51; P <0.001
4th Underlying dentin	**18.1±1.1 [Aa]**	**17.8±1.7 [Aa]**	**18.2±1.6 [Aa]**	Bonding type: F= 36.43; P <0.001
5th Underlying dentin	**18.9±1.9 [Aa]**	**19.3±1.4 [Aa]**	**19.2± 1.6 [Aa]**	Aging: F= 2.15; P <0.001
Res.IR				Interactions: F= 4.76; P < 0.001
1st Hybrid layer	**4.8±1.2 [Aa]**	**5.3±1.2 [Ab]**	**5.2±1.4 [Ab]**	
2nd Hybrid layer	**1.2±0.6 [Aa]**	**2.1±1.1 [Aba]**	**3.1±1.0 [Bc]**	**4th Underlying dentin**
3rd Bottom hybrid layer	**9.5±1.3 [Aa]**	**14.5±1.9 [Bb]**	**15.1±2.1 [Bc]**	Main effects: F= 19.35; P <0.001
4th Underlying dentin	**17.7±1.6 [Aa]**	**18.1±1.9 [Aa]**	**17.9±1.8 [Aa]**	Bonding type: F= 16.14; P <0.001
5th Underlying dentin	**18.8±1.3 [Aa]**	**19.1±1.1 [Aa]**	**19.3± 1.3 [Aa]**	Aging: F= 1.17; P <0.001
Res.IR/PLA				Interactions: F= 0.85; P 0.53
1st Hybrid layer	**4.9±1.1 [Aa]**	**5.1±1.0 [Ab]**	**5.1±1.9 [Ab]**	
2nd Hybrid layer	**1.6±0.5 [Aa]**	**5.4±2.2 [Bb]**	**6.2±2.3 [Bd]**	
3rd Bottom hybrid layer	**9.4±1.7 [Aa]**	**14.5±1.8 [Bb]**	**15.9±1.4 [Bc]**	
4th Underlying dentin	**17.8±2.3 [Aa]**	**17.7±2.1 [Aa]**	**17.6±1.9 [Aa]**	**5th Underlying dentin**
5th Underlying dentin	**19.9±1.1 [Aa]**	**19.4±1.4 [Aa]**	**19.5± 1.5 [Aa]**	Main effects: F=3.45; P=0.012
Res.IR/TMP+PLA				Bonding type: F=2.98; P=0.05
1st Hybrid layer	**4.9±1.1 [Aa]**	**5.0±1.6 [Ab]**	**5.1±2.2 [Ab]**	Aging: F=2.21; P=0.59
2nd Hybrid layer	**1.8±1.1 [Aa]**	**8.3±2.7 [Bc]**	**16.5±2.3 [Ce]**	Interactions: F=1.06; P= 0.41
3rd Bottom hybrid layer	**10.7±1.6 [Aa]**	**16.5±1.4 [Ac]**	**17.8±1.9 [Ad]**	
4th Underlying dentin	**18.1±1.8 [Aa]**	**18.2±2.1 [Aa]**	**18.3±1.7 [Aa]**	
5th Underlying dentin	**19.5±1.6 [Aa]**	**19.7±1.7 [Aa]**	**19.6± 1.4 [Aa]**	

For each vertical column: different lower case letter indicates differences between the tested adhesive procedure at the same indentation position ($p<0.05$).

For each row: different identical capital letter indicates differences between aging periods for the same adhesive procedure ($p<0.05$).

Table 2: Mean (MPa) and standard deviation (±SD) of microtensile bond strength (μTBS) values, percentage distribution of failure mode and percentage of beams tested or pre-load failed in each experimental group.

	24h (AS-aging)			90 days (AS-aging)		
	Mean (±SD)	[A/M/C] (%)	Tested/ Pre-Fail (%)	Mean (±SD)	[A/M/C] (%)	Tested/ Pre-Fail (%)
Res.CTR	39.5 (4.8) ^{A1}	5/85/10	100/0	26.8 (3.8) ^{A2}	40/60/0	100/0
Res.PLA	41.2 (3.8) ^{B1}	0/80/20	90/10	25.9 (5.8) ^{A2}	65/35/0	95/5
Res.TMP+PLA	36.0 (6.3) ^{A1}	10/85/5	95/5	19.3 (3.4) ^{A2}	45/55/0	100/0
Res.IR	35.3 (5.9) ^{A1}	5/85/10	95/5	23.5 (2.5) ^{A2}	35/65/0	90/10
Res.IR/PLA	37.1 (5.2) ^{A1}	5/85/10	85/15	21.2 (4.2) ^{A2}	30/70/0	80/20
Res.IR/TMP+PLA	31.4 (4.6) ^{A1}	10/90/5	95/5	28.1 (4.5) ^{A1}	20/80/0	100/0

For each horizontal row: values with identical numbers indicate no significant difference ($p>0.05$).

For each vertical column: values with identical letters indicate no significant difference using Student–Newman–Keuls test ($p>0.05$).

FIGURE 1: Schematic illustration of the specimen preparation, adhesive procedures, AFM nano-indentation and Raman microscopy evaluation.

Human third molars were used to prepare standardized dentin surfaces. The two different biomimetic primers were water solutions containing either poly-L-aspartic acid (PLA) alone or a combination of sodium trimetaphosphate plus PLA (TMP+PLA); deionized water was used as control pre-treatment. An ethanol-based resin primer and a control filler-free resin or an experimental ion-releasing resin containing a 40wt% Portland cement (calcium silicates) doped with β-TCP were applied onto the dentin surface and light-cured. After resin build-ups, the specimens were sectioned into slab and immersed in artificial saliva (AS) for different period times in order to evaluate the dentin remineralization at the resin-dentin interface through AFM nano-indentation and Raman microscopy [Image modification from Toledano *et al.,* (26)].

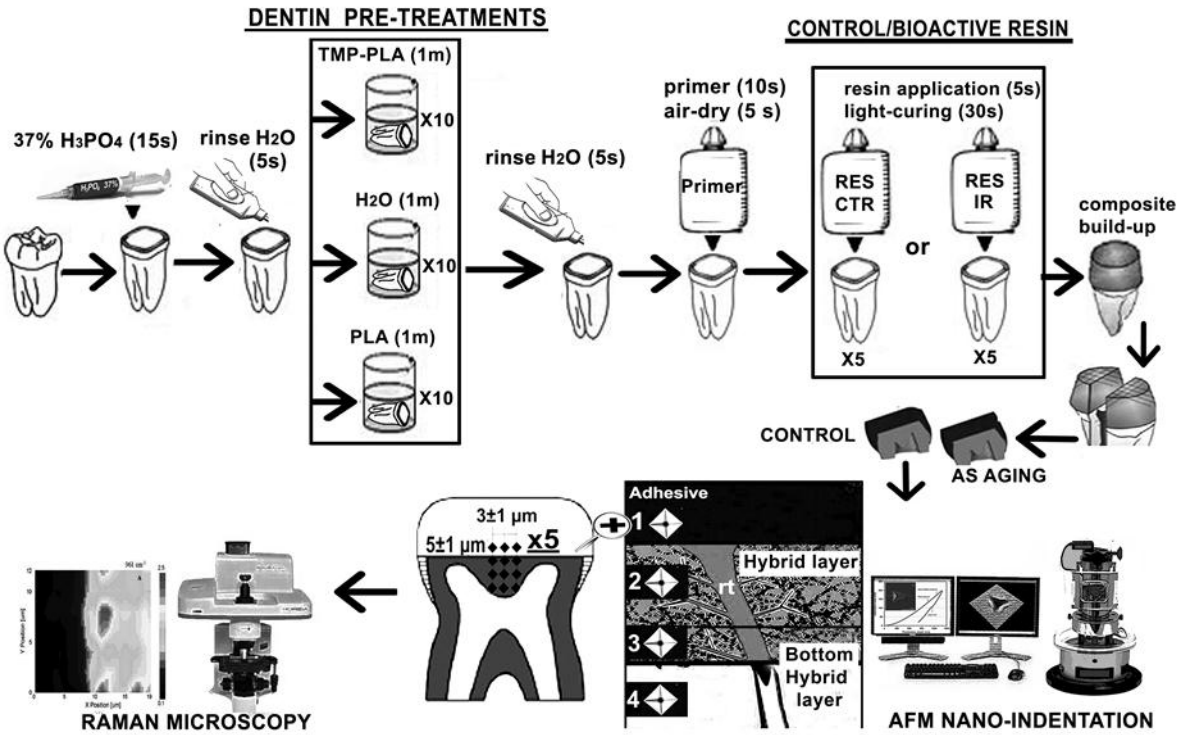

Figure 2. FTIR-ATR spectrum of acid-etched dentin treated with the experimental biomimetic solutions

TMP+PLA: the biomimetic primer containing poly-L-aspartic acid plus sodium trimetaphosphate. PLA: the biomimetic primer contains only poly-L-aspartic acid only. Primer: control resin co-monomer primer formulated using UDMA, BisGMA, TEGDMA HEMA and 50vol% absolute ethanol. Note the phosphate uptake by the demineralized collagen induced by the biomimetic primer TMP+PLA or PLA (1083 and 1034 cm^{-1}) and the increase of vibration of P-O at 967 cm^{-1} indicating more presence of phosphate.

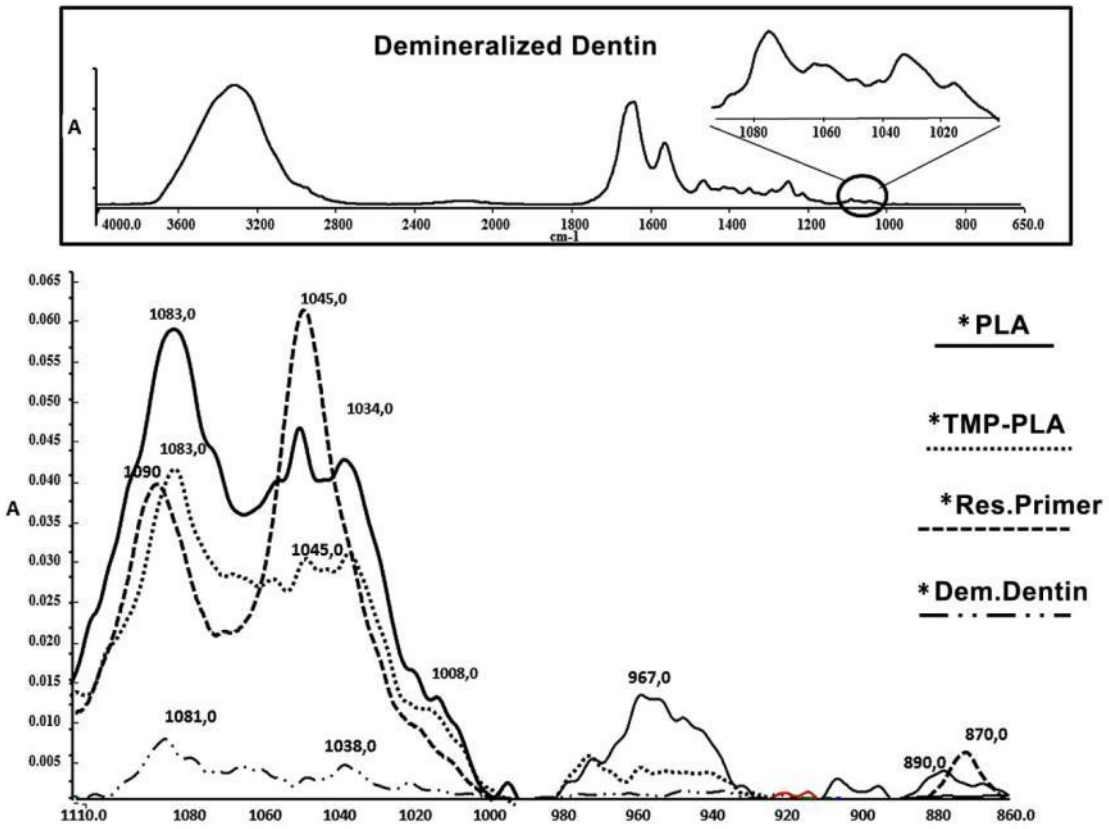

Figure 3. CLSM and AFM images of resin-dentin interface after 24 h storage

A: CLSM 3D projection image captured in reflection/fluorescence showing the resin-dentin interface created with the experimental Res.IR. It is possible to see a strong reflection signal from the submicron filler particles within the adhesive layer (ad+FL) and inside the dentinal tubules (t). A clear micropermeability signal can be seen at the hybrid layer (HL). The brighter the fluorescein fluorescence, the higher the micropermeability of water throughout the hybrid layer.

B: CLSM 3D projection image (reflection/fluorescence) of the resin-dentin interface created with the control resin containing no filler. In this case it is possible to note strong micropermeability within the hybrid layer (HL). There was no reflection signal is shown as there is no filler particles within the adhesive layer (ad) or inside the dentinal tubules (t).

C: AFM topographic image showing the indentations performed in straight lines along the hydrated resin-dentin interface created with the experimental Res.IR/PLA starting from the top of the hybrid layer (HL). The second indentation made in the middle of the hybrid layer (HL) and the third in the bottom of the hybrid layer (bHL). The remnant indentations (pointer) were performed within the underlying mineralized dentin (d). It is also possible to see the presence of 5-to-10 μm diameter filler particles (FL) within the adhesive layer (ad).

D: AFM topographic image showing the indentations in the resin-dentin interface created with the experimental Res/PLA starting from the top of the hybrid layer (HL). Also in this case the second indentation was performed in the middle of the hybrid layer (HL) and the third on the bottom of the hybrid layer (bHL). It is also possible to see the resin composite (c) layer above of the hybrid layer (HL) and underlying mineralized dentin (d); this latter characterized by the presence of resin tags (rt).

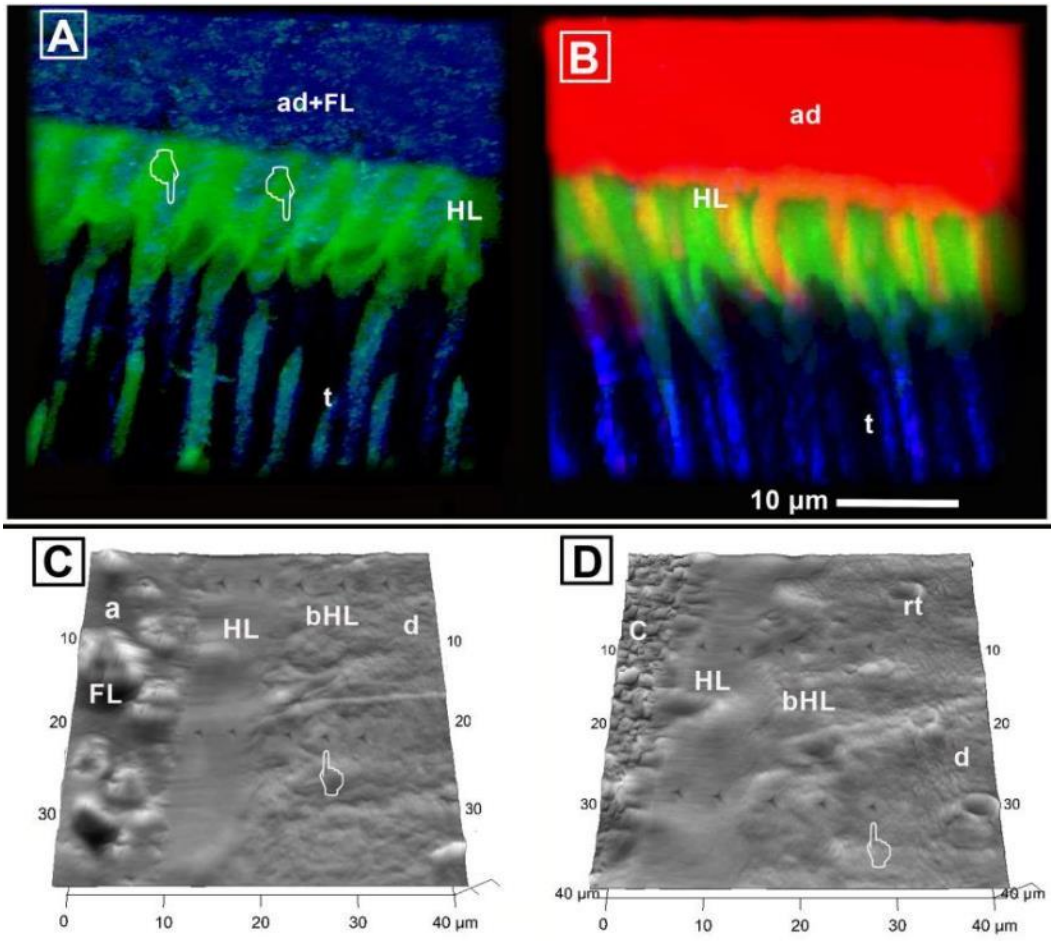
A
ad+FL
HL
t
B
ad
HL
t
10 µm
C
a
HL
bHL
d
FL
10
20
30
0
10
20
30
40 µm
D
rt
C
HL
bHL
d
10
20
30
40 µm
0
10
20
30
40 µm

Figure 4. CLSM images of the resin-dentin interfaces after 90 days of AS storage

A: CLSM single projection showing the resin-dentin interface created with the control resin (Res.CTR). It is possible to note the presence of a degraded hybrid layer (arrow) created by aging degradation of collagen matrix, but the presence of remnant resin tags (rt) between the adhesive layer (a) and the dentin; this latter is characterized by the presence of multiple dentinal tubules (t). Only a slight micropermeability can be only observed at the bottom of the hybrid layer (fluorescein emission).

B: CLSM single projection showing the resin-dentin interface created with the resin control applied onto the dentin pre-treated with the polyaspartic acid primer (Res.PLA). Also in this case the hybrid layer was affected by degradation which created a clear gap within the interface with remnant resin tags (rt) between the adhesive layer (a) and the dentin. Micropermeability can be also detected at the bottom of the hybrid layer.

C: CLSM single projection showing the resin-dentin interface created with the filler-free control resin applied to the dentin pre-treated with the solution containing sodium trimetaphosphate and polyaspartic acid (Res.PLA+TMP). Also in this case the hybrid layer was affected by degradation which created a clear gap within the resin-dentin interface. Again, micropermeability is only detected at the bottom of the hybrid layer (fluorescein emission).

D: CLSM single projection showing the resin-dentin interface created with the experimental ion-releasing (Res.IR) applied onto acid-etched dentin. The hybrid layer is partially affected by micropermeability (arrow) due to mineral deposition (reflection signal). An intense reflection signal (*mineral presence) can be also seen within the adhesive layer (a).

E: CLSM single projection showing the resin-dentin interface created with the experimental ion-releasing (Res.IR/PLA) applied onto the dentin pre-treated with the polyaspartic acid primer. The resin-dentin interface is characterized by slight micropermeability (arrow) due to minerals deposited within the hybrid layer (reflection signal). An intense reflection signal (*mineral presence) can be also seen within the adhesive layer (a), while underneath the HL there is the presence of resin tags (rt), (rhodamine B emission).

F: CLSM single projection showing the resin-dentin interface created with the experimental ion-releasing (Res.IR/PLA+TMP) applied onto the dentin pre-treated with the primer containing trimetaphosphate and polyaspartic acid. The resin-dentin interface presents a weak micropermeability signal (arrow) but a hybrid layer completely mineralized (reflection signal). Also in this case it is possible to see an intense reflection signal (*mineral presence) within the adhesive layer (a). An intense reflection signal (*mineral presence) can be also seen within the adhesive layer (a) and resin tags (rt) underneath the HL.

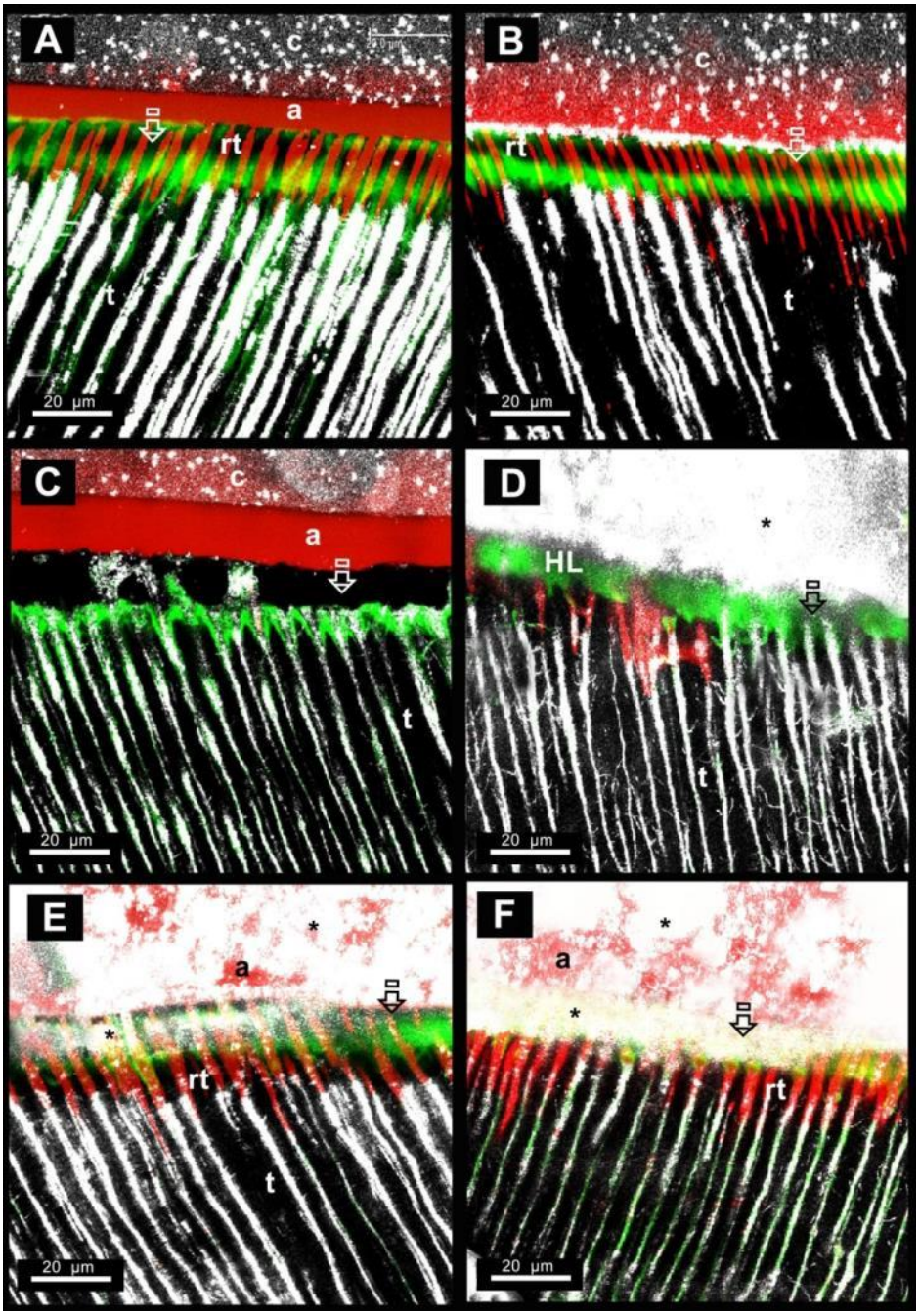
A
c
a
rt
t
20 µm
B
c
rt
t
20 µm
C
c
a
t
20 µm
D
*
HL
t
20 µm
E
*
a
*
rt
t
20 µm
F
*
a
*
rt
20 µm

Figure 5. AFM topographic image of resin-dentin interfaces after 90 days of AS storage

A: AFM image showing the resin-dentin interface created with the filler free control resin (Res.CTR) after 90 days of AS storage. The presence of a gap (pointer) between the hybrid layer (HL) and bottom of hybrid layer (bHL) is noticed, probably due to collagen fibrils degradation processes. A less evident gap may be seen between HL and the adhesive layer (a).

B: AFM image showing the resin-dentin interface created with the experimental ion-releasing (Res.IR), after 90 days of AS storage. The hybrid layer (HL) is well defined with no signs of degradation.

C: AFM image showing the resin-dentin interface after 90 days of AS storage created with the experimental ion-releasing (Res.IR/PLA) applied onto the dentin pre-treated with the polyaspartic acid primer. It is possible to see that the hybrid layer (HL) has no sign of degradation and adhesive layer (a) and the presence of the filler within the adhesive layer (a).

D: AFM image showing the resin-dentin interface after 90 days of AS storage created with the experimental ion-releasing (Res.IR/PLA+TMP) applied onto the dentin pre-treated with the polyaspartic acid and sodium trimetaphosphate primer. The hybrid layer (HL) is only partially visible in the proximity of the adhesive layer (a) due to the high level of remineralization achieved at the middle of the hybrid layer and bottom of hybrid layer; indeed, these latter areas of the bonding interface are indistinguishable from the underlying in dentin (d).

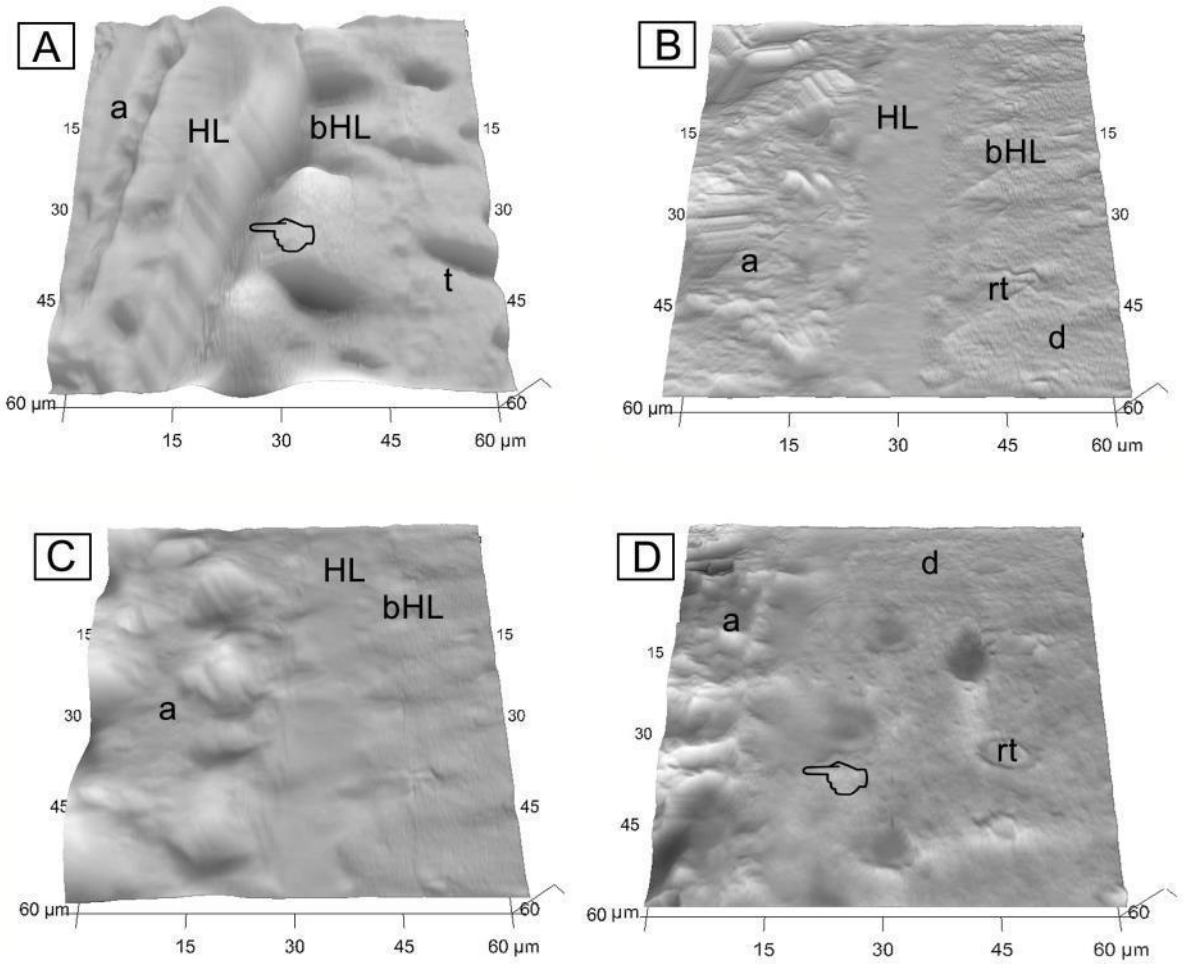

Figure 6. - Raman spectroscopic cluster analysis with mean and standard deviations and images of the mineral matrix ratio of the principal components.

Clusters analysis of principal components identified before and after storage [sound dentin (A), demineralized dentin at the bottom of the hybrid (B), hybrid Layer Res.CTR, (C) and hybrid Layer Res.IR (D)] of the specimens created using the Res.CTR (A) or Res.IR (B) with or without the pre-treatments using the two biomimetic primers tested in this study (PLA and TMP+PLA).

E and F: Mean and standard deviations of the mineral matrix ratio (MMR) between the phosphate [v_1 - 961 cm^{-1}] P–O symmetric stretch and collagen [1465 cm^{-1}, CH_2 deformation] of each principal component identified by the cluster analysis before and after prolonged storage.

Significant differences of each similar cluster component after the 90 days remineralization periods (*). Significant differences between the tested remineralizing bonding procedures at the same cluster component (^).

Raman spectroscopic images of the intensity ratio of the phosphate (961 cm^{-1}) to collagen (1452 cm^{-1}) for the specimens in groups Res.IR/PLA+TMP and Res.IR/PLA.

(G) Res.IR/PLA+TMP after 24h of AS storage, high gradient of mineralization only at the underlying dentin (d), but not along the bonded interface (i) are shown.

(H) After 90 days immersion in AS, is evidenced at the specimens of this group (Res.IR/PLA+TMP) specimens show pronounced mineralization both at the underlying dentin (d) and along the bonded interface (i); some areas at the interface show lower remineralization (pointer), probably due to the presence of resin infiltration.

(I) After 24h of AS storage, Res.IR/PLA specimens presented high mineralization only at the underlying dentin (d), but not along the bonded interface (i).

(L) The specimens created using the Res.IR/PLA and immersed in AS for 90 days showed high mineralization at the underlying dentin and low mineralization (pointer) along the bonded interface (i).

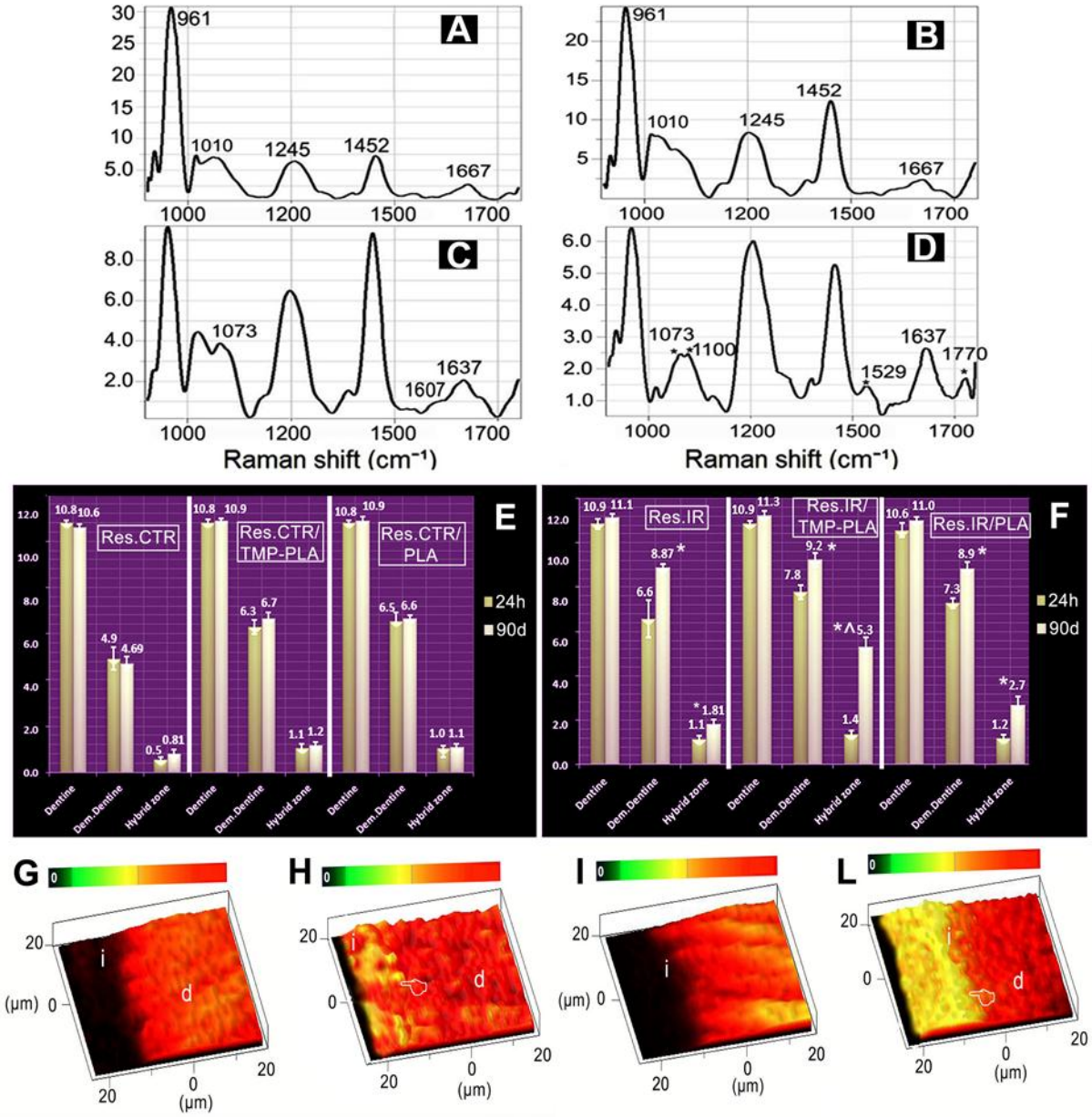
A
961
1010
1245
1452
1667
B
961
1010
1245
1452
1667
C
1073
1607
1637
D
1073
1100
1529
1637
1770
Raman shift (cm⁻¹)
Raman shift (cm⁻¹)
E
Res.CTR
Res.CTR/ TMP-PLA
Res.CTR/ PLA
24h
90d
Dentine
Dem.Dentine
Hybrid zone
F
Res.IR
Res.IR/ TMP-PLA
Res.IR/PLA
24h
90d
G
H
I
L
(μm)

Figure 7. Scanning electron microscopy images of debonded resin-dentin specimens created using the different bonding approaches and tested after 24 h of AS storage.

(A) Low magnification micrograph (X2,000) of the control resin (Res.CRT no filler) bonded to dentin which failed in mixed mode (mixed). Note remnant resin (ad) on debonded surface and the presence of dentinal tubules (dt) occluded by resin tags (rt). **(B)** At higher magnification, (X30,000) note the presence of remnant collagen fibrils, which may indicate that the debonding fracture occurred at the bottom of the hybrid layer (pointer).

(C) Micrograph (X2,000) of the specimens bonded with Res.CRT/PLA debonded in mixed mode. Note the presence of dentinal tubules (dt) partially or completely occluded by resin tags as well as remnant resin (ad). **(D)** At higher magnification (X30,000), Note patent dentinal tubule (dt) and very few remnant collagen fibrils (pointer) which indicate good resin infiltration of the demineralized dentin, the debonding fracture occurred beneath the bottom of the hybrid layer (pointer).

(E) Micrograph (X2000) of the specimens bonded with Res.CRT/TMP+PLA; about half of the dentinal tubules (dt) were partially or completely occluded by resin tags. **(F)** At higher magnification (X30,000), observe the presence of a pulled-out resin tag (rt) and an important presence of intact collagen fibrils (pointer). It indicates a lack of resin infiltration within the demineralized dentin.

(G) Micrograph (X20,00) of the mixed failure mode of the ion-releasing resin (Res.IR) bonded dentin. Note the presence of open dentinal tubules (dt) and remnant resin (ad) on the dentin surface. **(H)** At higher magnification (X30,000), the presence of remnant collagen fibrils and fractured resin tags inside the tubules, indicating that the debonding fracture occurred at the bottom of the hybrid layer (pointer).

(I) Micrograph (X2,000) of the failure mode of the experimental resin Res.IR/PLA bonded to dentin. The dentin surface is covered by resin (ad); resin surface shows voids where the ion-releasing fillers pulled out (*). **(L)** In this image is observable at higher magnification (x30,000) the dentin surface covered by a resin layer (ad) characterized by voids left by the debonding of the ion-releasing filler particles (pointer) from the adhesive resin.

(M) Micrograph (X2,000) of the failure mode of the resin Res.IR/TMP+PLA bonded to dentin. The dentin surface and the dentinal tubules (dt) are still covered by resin (ad); this latter is characterized by the voids created by the ion-releasing fillers (*). **(N)** At higher magnification (X30,000), note the dentin surface covered by a resin layer (ad) and characterized by the multiple voids left by the loss of ion-releasing filler particles. In the dentin bonded with both Res.IR/PLA and Res.IR/TMP+PLA, the fracture occurred mainly above the hybrid layer.

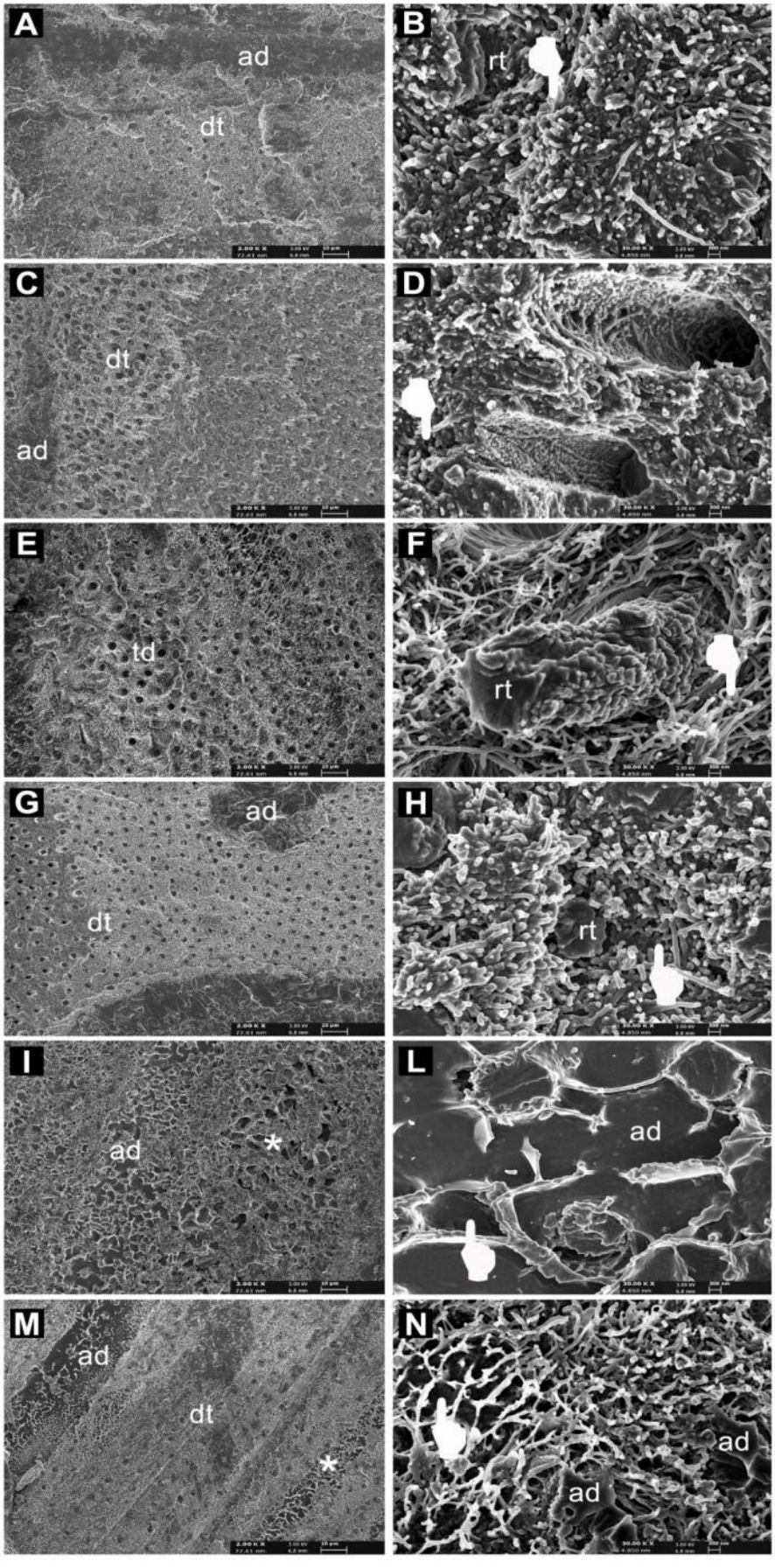
A
ad
dt
B
rt
C
dt
ad
D
E
td
F
rt
G
ad
dt
H
rt
I
ad
*
L
ad
M
ad
dt
*
N
ad
ad

Figure 8. Scanning electron microscopy images of debonded resin-dentin specimens created using the different bonding approaches and tested after 90 days of AS storage.

(A) High magnification image (X15,000) showing a control resin (Res.CTR)-bonded specimen that failed in adhesive mode. No remnant collagen fibrils are observable due to the collagen degradation process and no mineralization of either intertubular (*) or intratubular dentin (itr) is noticed; fractured resin tags are still present inside tubules.

(B) High magnification image (X15,000) showing an specimen from resin Res.CTR/PLA group that failed in adhesive mode, note few remnant collagen fibrils (pointer), as result of collagen degradation with no clear mineral precipitation in either the intertubular (*) or intratubular dentin (itr). Fractured resin tags are still present in dentin tubules (rt).

(C) High magnification image (X15,000) showing a specimen from Res.CTR/TMP+PLA group that failed in adhesive mode. Some remnant collagen fibrils (pointer) on the dentin surface are observable but no clear mineral precipitation is noticed. Fractured resin tags are present inside the dentin tubules (rt).

(D) In this lower low magnification (X2,000) micrograph of a debonded specimen created with the experimental ion-releasing resin (Res.IR) observe fractured resin tags (rt) occupying most tubules. At higher magnifications (X15,000) and (X30,000) **(E and F respectively)** it is possible to see the resin tags (rt) and the dentin surface covered by minerals with no sign of exposed collagen fibrils (pointer) both in intratubular (irt) and intertubular (*) dentin.

(G) Low magnification (X2000) micrograph of a debonded specimen created with the resin Res.IR/PAL. Several resin tags (rt) are shown. At higher magnifications (X15,000) and (X30,000) **(H and I respectively)** these resin tags (rt) and the dentin surface appear mainly covered by minerals with no sign of exposed collagen fibrils (pointer). Both the dentin bonded with Res.IR and Res.IR/PLA fractured mainly beneath the hybrid layer.

(L) SEM micrograph (X15,000) of a debonded specimen created using the resin Res.IR/TMP+PAL, showing completely mineralized dentin surface with broken resin tags (rt) at the dentinal surface. At higher magnification (X15,000) **(M)** the presence of minerals and the absence of exposed collagen fibrils on this dentin surface is clearly observed (pointer). **(N)** Nano-crystals deposition (pointer) on the collagen fibrils of the intertubular (*) and intratubular dentin (itr) can be clearly seen at higher magnification (X55,000)**.**

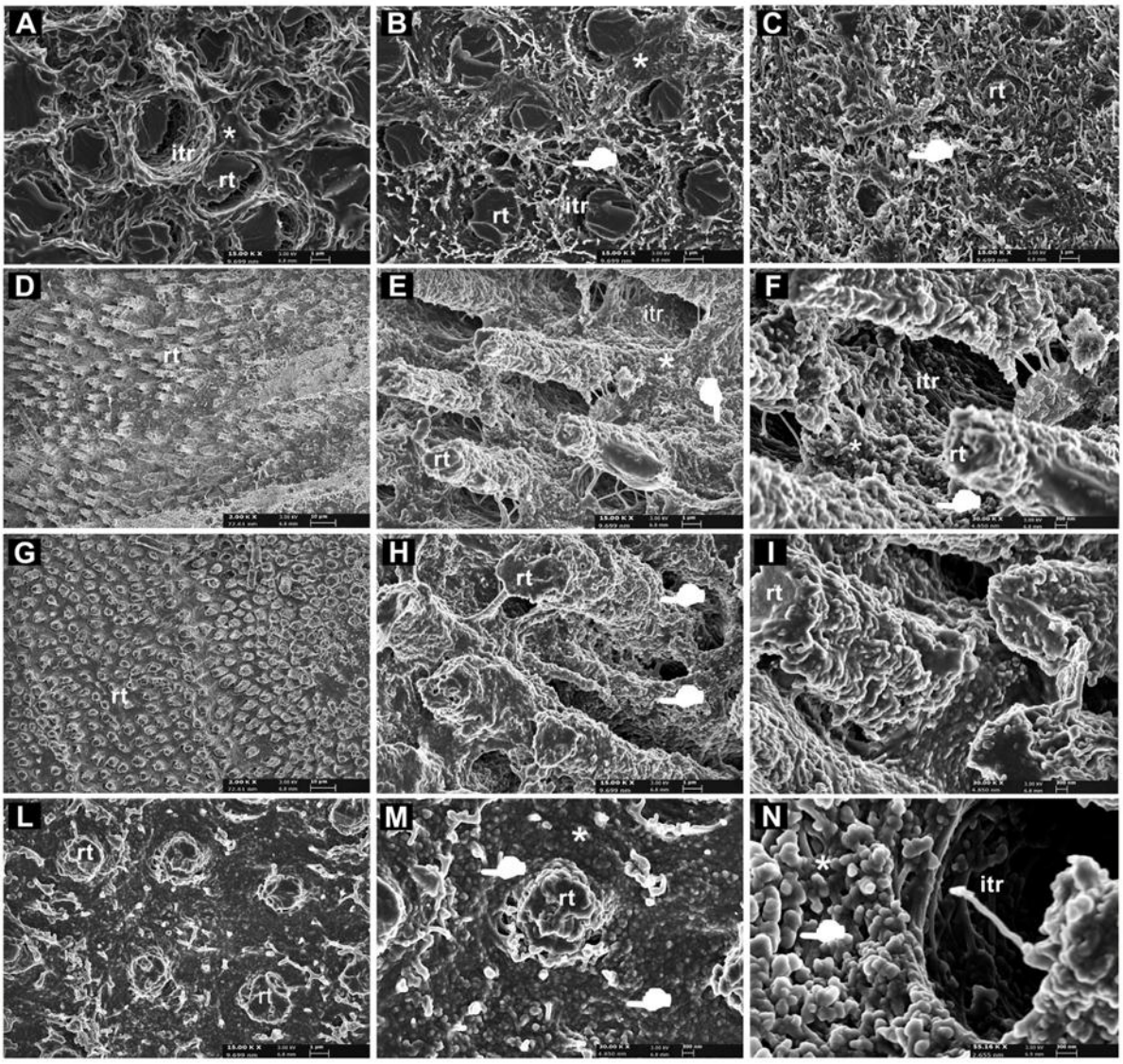
A
itr
*
rt
B
*
rt
itr
C
rt
D
rt
E
itr
*
rt
F
itr
*
rt
G
rt
H
rt
I
rt
L
rt
rt
M
*
rt
N
*
itr